Universidad
Tecnológica
de Pereira

MASTER'S PROGRAM IN ELECTRICAL ENGINEERING

THESIS PRESENTED AS A PARTIAL REQUIREMENT TO QUALIFY FOR THE MASTER'S DEGREE IN ELECTRICAL ENGINEERING

WIND-SOLAR-HYDROTHERMAL DISPATCH USING CONVEX OPTIMIZATION

Juan Camilo Castaño Guzmán

supervisor
Alejandro GARCÉS

March 2020

Abstract

In this research a convex optimization methodology is proposed for the Short-term hydrothermal scheduling (STHS). In addition, wind and solar generation are also considered under a robust approach by modeling the equilibrium of power flow constraint as chance box constraints, which allows determining the amount of renewable source available with a specific probability value. The proposed methodology guarantees global optimum of the convexified model and fast convergences. The methodology is evaluated under three circumstances: First, the conventional hydrothermal coordination is compared with the existing results in the scientific literature, most of the previous results are metaheuristics. The presented methodology demonstrated to be highly accurate and fast. Second, the deterministic model that considers the grid, wind and solar generation is evaluated under two cases: high capability of the lines and low capability of the lines. Simulations demonstrates how the capability of the grid affects the scheduling of generation units. Finally, a convex-robust model is evaluated considering the stochasticity of the load, wind and solar sources. The test results reveal how the scheduling, with renewable resources, depends considerably on the level of desired robustness.

Acknowledgment

I would first like to thank my thesis advisor, professor Alejandro Garcés of the Department of Electric Power Engineerig at Universidad Tecnológica de Pereira, who guided me throughout this project. I would also like to acknowledge Professor Olav B. Fosso from Norwegian University of Science and Technology for his invaluable comments and suggestions about the short term hydrothermal coordination.

Contents

1 Introduction **12**
- 1.1 Motivation . . . 12
- 1.2 Problem statement . . . 14
- 1.3 State of the Art . . . 15
- 1.4 Contributions . . . 19
- 1.5 Document organization . . . 19

2 Deterministic Mathematical Model **20**
- 2.1 Modeling components . . . 20
  - 2.1.1 Thermal units . . . 20
  - 2.1.2 Hydro units . . . 22
  - 2.1.3 Wind units . . . 23
  - 2.1.4 Solar photovoltaic units . . . 25
  - 2.1.5 Classic short-therm hydrothermal dispatch model (Model I) 25
  - 2.1.6 DC powerflow . . . 29
  - 2.1.7 STHS with wind and solar resources . . . 30
- 2.2 Convex qualification and challenge of the model . . . 30

3 Second-order cone programming for the STHS **31**
- 3.1 The second order cone . . . 31
- 3.2 Quadratically constrainted quadratic programming problems . . . 32
- 3.3 Quadratically constraint rewritten as second-order cone constraint 33
- 3.4 Convex approximation for the STHS model . . . 34
- 3.5 Convex model of STHS (Model II) . . . 35
- 3.6 Convex model of STHS considering the grid (Model III) . . . 37
- 3.7 Deterministic convex model of STHS considering the grid and renewable sources (Model IV) . . . 40

4 Robust model **43**
- 4.1 Probability concepts . . . 44
  - 4.1.1 Deterministic and random variables . . . 44
  - 4.1.2 Probability space . . . 44
  - 4.1.3 Probability density function . . . 44
  - 4.1.4 Cumulative distribution function. . . . 44

4.1.5 Quantile function 46
4.2 Robust optimization 46
4.3 Chance box constraint 48
4.3.1 Chance box constraint definition 49
4.3.2 Considering stochasticity of renewable sources into the STHS 50
4.3.3 Flow balance as a chance box constraint 50
4.4 Stochasticity of the radom variables 51
4.4.1 Stochastic behavior of wind and wind power data 51
4.4.2 Stochasctic behavior of solar power data 53
4.4.3 Stochasctic behavior of load 53
4.5 Robust hydrothermal-wind-solar coordination model (Model V) . 54

5 Results **57**
5.1 Results Model II 58
5.2 Results Model IV 58
5.3 Results Model V 63
5.4 Other results 66
5.5 Summary of results 74

6 Conclusions and future works **77**
6.1 Conclusions 77
6.2 Future works 78

Appendixes **78**

A Test system **79**
A.1 Characteristics of load, hydro and thermal units 79
A.2 Characteristic of wind and solar farms 80
A.3 Characteristics of grid 81

B Brief review of convex optimization **86**
B.1 Convex set 86
B.2 Convex function 87
B.3 Convex problem 87
B.4 Uniqueness and globality 87

C Probability space definitions **89**
C.1 Sample space H 89
C.2 Outcomes and events 89
C.3 $\sigma-$algebra $\mathfrak{B}$ 89
C.4 Probability measure function $\mathfrak{P}$ 90

D linearization of the problem **91**

Nomenclature

$F_L^{k,n,t}$	Power flow through the line connected between node k and node n at moment t
$[\theta]$	Vector of angular differences
$[B]$	Nodal admitance matrix
$[F_{P_D}^{-1}(\zeta)]^t$	Vector of quantile values of demand at moment t
$[P]$	Vector of active injected powers
$[P_D]$	Vector of powers consumed
$[P_G]$	Vector of powers generated
α^i	Coefficients of fuel cost function of ith thermal unit
β^i	Coefficients of fuel cost function of ith thermal unit
β_p	pitch angle
Δ	Set of all thermal units
$\emptyset$	Empty set
η	Efficient of turbine
γ^i	Coefficients of fuel cost function of ith thermal unit
κ_w	Shape coefficient Weibull distribution of wind
Λ	Swept area by wind generator blade
λ_{tip}	Tip-speed ratio
$\mathcal{M}$	Uncertainty set
$\mathfrak{B}$	$\sigma-$algebra
$\mathfrak{B}$	Subset of 2^H
$\mathfrak{P}$	Probability measure function

$\mathfrak{U}$	Auxiliary variable
$\mathfrak{X}$, $\mathfrak{Y}$, $\mathfrak{Z}$	Points of a convex function
$\overline{P_D}$	Load forecast
π	Index of upper reservoir
ψ	Solar irradiation
ρ	Density of water
ρ_{air}	Air density
τ	Time delay to immediate downstream plant
$\theta^{k,n,t}$	Angular differences between node k and n at moment t
θ_{kn}	Angular difference between nodes k and n
ϱ	Constants of an affine constraint
ζ_t	Probability to hold a constraint at moment t
$a^\top$	Coefficient vector of the constraint of a robust problem
$A^\top A$	Constant of a quadratic constraint
A_0	Constant of the quadratic objective function
A_i	Coefficient matrix of a second order cone constraint
a_i	Bounds of a box constraint
B	Subset of $\mathfrak{P}$
b	Constant of a constraint of a robust problem
b_i	Coefficient vector of a second order cone constraint
$c^\top$	Coefficient vector of the objective function or a robust problem
C_1^j, C_2^j, C_3^j	Hydropower generation coefficients of jth hydro unit
C_4^j, C_5^j, C_6^j	Hydropower generation coefficients of jth hydro unit
c_i	Coefficient vector of a second order cone constraint
C_p	Power coefficient of wind unit
c_w	Scale coefficient Weibull distribution of wind
C_{F_s}	Capacity factor of solar power plant
$C_{F_s}^{u,t}$	Capacity factor of unit u at moment t

d	Constant of a quadratic constraint
d_0	Constant of the quadratic objective function
d_i	Constant of a second order cone constraint
D_t	Deterministic variable at moment t
e	Index of wind unit
E_p	Gravitational potential energy
E_S	Energy produced by solar unit
$E_{S_{rated}}$	Rated energy produced by solar unit
$F(x)$	Cumulative distribution function
$f(x)$	Probability density function
$f^\top$	Coefficient vectors of the objective function
f_0	Objective function
$F_{Ft}^{k,t}$	Flow through the primary of the transformer located at node k at moment t
$F_{L_{Tmax\ P.U}}^{k,n}$	Minimum thermal limit of the line between nodes k and n
$F_{L_{Tmin\ P.U}}^{k,n}$	Maximum thermal limit of the line between nodes k and n
$F_L^{k,n,t}$	Flow through the line between nodes k and n at moment t
$F_{P_D^{k,t}}$	Cumulative distribution function of the demand of node k at time t
$F^{-1}_{P_D^{k,t}}$	Quantile function of the power demanded by the node k at moment t
$F_{P_G^{k,t}}$	Cumulative distribution function of the power generated at node k at moment t
$F^{-1}_{P_G^{k,t}}$	Quantile function of the power generated at node k at moment t
$F_{St}^{k,t}$	Flow through the secondary of the transformer located at node k at moment t
F_{X_t}	Cumulative distrbution function of random variable R at moment t
$F^{-1}_{X_t}$	Quantile function of random variable R at moment t
g	Acceleration due to gravity
$g(x)$	Objective function

H	Sample space
h	Height of the reservoir with respect to powerhouse
h_H	Headwater level
h_L	Altitude reduction due to the losses produced by the civil structures
i	Index of thermal units
$I^{j,t}$	Water inflows of reservoir j at moment t
j	Index of hydro units
k	Node
l_i	Bounds of a box constraint
m	Mass of water
n	Node connected to the node k
N_k	Group that consists of nodes connected to the k node
o	Parameter of an uniform distribution
$P^k_{H_L}$	Hydropower of unit k using the linearized equation
$P^k_{H_Q}$	Hydropower of unit k using the quadratic equation
P_0	Coefficient matrix
$P^{k,t}_D$	Power consumed by the load located at node k at moment t
P^t_D	Total power demanded by the system at moment t
P_e	Wind power
$P^{k,t}_G$	Power produced by the generator located at node k at moment t
P_i	Coefficient matrix
$P_i^{-1/2}$	Cholesky decomposition
$P_i^{1/2}$	Cholesky decomposition
P_S	Power produced by solar unit
$P^{k,t}_s$	Power produced by solar generator located at node k at moment t
$P^{u,t}_S$	Power produced by uth solar unit at moment t
P_w	Power produced by a wind unit
$P^{e,t}_w$	Power produced by eth wind unit at moment t

$P_w^{k,t}$ Power produced by wind unit located at node k at moment t

$P_H^{j.t}$ Power produced by jth hydro unit at moment t

P_{kn} Power flow between nodes k and n

$P_{S_{rated}^u}$ Rated power of uth solar unit

$P_{Th}^{i,t}$ Power produced by ith thermal unit at moment t

$P_{w_{rated}}$ Rated power of wind turbine

Q Water flow

$Q(p)$ Quantile function

$Q^{j,t}$ Discharged water by hydro unit j at moment t

q_0 Vector of coefficients

q_i Vector of coefficients

r Constant of a quadratic constraint

r_0 Constant of the quadratic objective function

s Parameter of an uniform distribution

$S^{j,t}$ Spillage of reservoir j at moment t

S_T Studied time interval

S_{Ω^j} Set of upper reservoirs of reservoir j

S_H Set of all hydro units

t, T Index of time intervals, with T being the last

TP_{H_L} Total hydropower by using the linearized equations

TP_{H_Q} Total hydropower by using the quadratic equations

U Coefficient vector of an affine constraint

u Index of solar unit

$V^{j,t}$ Water volume of reservoir j at moment t

v_w Wind speed.

$v_w^{e,t}$ Wind speed data for eth unit at moment t

v_{cut-in} Cut-in speed of the wind turbine

$v_{cut-out}$ Cut-out speed of the wind turbine

$v_{rated\ data}$ Rated value of wind data

v_{rated} Rated wind speed of a wind turbine

X_t Random variable at moment t

X_{kn} Series reactance between nodes k and n

Y Set of variables of an optimization problem

z Auxiliary variable of an optimization problem

APSO Adaptive particle swarm optimization

BCGA Binary coded genetic algorithm

CDE Chaotic differential evolution

CDEA Adaptive chaotic differential evolution algorithm

CEP Evolutionary programs with Gaussian mutation

CPSO Couple based particle swarm optimization

DE Differential evolution technique

DRQEA Differential real-coded quantum-inspired evolutionary algorithm

EGA Enhanced genetic algorithm

EPSO Enhanced particle swarm optimization

ERWCA Evaporation rate–based water cycle algorithm

FEP Evolutionary programs with Cauchy mutation

GA Genetic algorithms

IFEP Evolutionary programs with Gaussian and Cauchy mutation

INF Infimum

IPSO Improved particle swarm optimization

LCSO Local vision of particle swarm optimization with constriction factor

LP Linear programming

LWPSO Local vision of particle swarm optimization with inertia weight

MAPSO Modified adaptive particle swarm optimization

MDE Modified differential evolution algorithm

MDNLPSO Modified dynamic neighborhood learning based particle swarm optimization

MHDE Modified hybrid differential evolution algorithm

PDF Probability density function

HPDLQ Hydropower difference between linear equations and quadratic equations

Prob Probabilitiy of ocurrence of an event

PSO Particle swarm optimization

QCQP Quadratically constrainted quadratic programming

QRSOS Quasi-reflected symbiotic organisms search algorithm

RCGA Real coded genetic algorithm

RO Robust optimization

SDP Semidefinite programming

SIN Sine

SO Stochastic optimization

SOC Second-order cone

SOS symbiotic organisms search algorithm

SPPSO Small population based particle swarm optimization

SPPSO Small population based particle swarm optimization

STHS Short-term hydrothermal scheduling

SUP Supremum

TLBO Teaching learning based optimization algorithm

Chapter 1

Introduction

1.1 Motivation

Economical growing of modern societies depends highly on their capacity to produce goods and services by using electrical power. Unfortunately, this massive use of electric power has produced strong environmental impacts which can put at risk the continuity of the humankind in the earth. One of the most harmful effects that the human beings have had on nature is the accumulation of greenhouse gasses in the atmosphere, where the electricity production sector is responsible for nearly 25% of global green house gasses emissions (Spandan Thaker and Kumar, 2019). A transition from fossil fuels based sources to renewable alternatives is necessary to keep the economical growing and meet the green house gasses emission reduction targets. In addition, the advent of renewable technologies reduces the operation cost of these units, since the fuel cost is zero.

In order to carry out this transition, modern power systems seek to introduce more renewable resources into the energy mix, however, there is a renewable resource already available massively in conventional power systems namely, the hydroelectric generation. This type of generation is abundant in countries like Norway, Colombia and Brazil, and are called to be the main energy storage for the interconnected system (Isabela Alves de Oliveira and Szklo, 2017) (del Mar Rubio and Tafunell, 2014) (Ruud Egging, 2016). Notice that using renewable energy resources does not mean that the conventional generators are going to disappear completely. Actually, the completely replacement of traditional generation sources (e.g thermal and hydro power) seems to be an Utopian scenario, at least in the short and medium term. Instead, a scenario with a partial penetration of renewable sources is more plausible (UPME, 2019).

Integrating these new technologies in the traditional system requires operation strategies that consider the peculiarities of these power units in order to

guarantee the stable and reliable operation of the system under variations in the load/generation in the short, medium and long time. This implies that more efficient short-term hydrothermal coordination model that considers the presence of these new technologies (mainly wind and solar) need to be proposed.

The short-term hydrothermal coordination is complicated by itself since it is usually a deterministic non-linear problem (Kothari and Dhillon, 2007). Therefore, the problem is related with the high non-linearity and non-convexity of the model. Even though this problem has been widely studied, most of research have used linearizations and heuristic algorithm in order to deal with the non-linear and non-convex structure of the problem. These methods face two main problems: On one hand, heuristics are characterized by the lack of understanding of the mathematical structure of the problem, the randomness of their results and their high computational burden, which is not suitable for real time operation. On the other hand, linearizations produce loss of information in the model that can result in nonfeasible operation points (See appendix D). Moreover, when other renewable resources are considered, the problem is not only non-linear/non-convex but also stochastic, since wind speed and solar radiation cannot be predicted accurately. That is a why a methodology that considers the original structure of the problem and the stochasticity of renewable resources is required in order to operate the power systems optimally.

This research presents a short-term hydro-wind-solar-thermal coordination model where the non-convexity of the problem is dealt by proposing a second-order cone (SOC) approximation. The stochasticity of the renewable sources is considered by proposing a robust model where the equilibrium power flow constraints are modeled as chance box constraints. This makes sense if it is supposed that there is no a correlation between solar irradiation, wind speed and water inflows.

There are several advantages formulating a problem as a convex optimization problem. For instance, it is possible to guarantee global optimum of the convexified model. In addition, convex optimization guarantees convergence by using interior point-methods or other special methods. These solution methods are reliable enough to be embedded in a real-time reactive or automatic control system. There are also conceptual advantages of formulating a problem as a convex optimization problem. The dual problem, often has an interesting interpretation in terms of the original problem, and sometimes leads to an efficient or distributed method for solving it.

Among convex optimization models, stand out second-order cone programming, which is a branch of convex optimization which has proved to be useful for dealing with linear programs, convex quadratic programs, quadratically constrained quadratic programs (QCQP) and many other problems that do not fall into these three categories. Its name arises from the constraints, which are equivalent to requiring the affine functions to lie in the second-order cone in

$\mathbb{R}^{k+1}$. The main advantage of modeling a problem as a second order cone problem stems from its faster convergence compared to other convex optimization techniques (Boyd and Vndenberghe, 2009) (Alizadeh and Goldfarb, 2003) (see Chapter 3).

On the other hand, optimization problems that contain uncertain data can be faced under two approaches, namely stochastic and robust optimization. Stochastic optimization requires that the true probability distribution of random data has to be known in order obtain a computationally treatable problem. On the other hand, robust optimization does not require to know the probability distributions of data, but instead it assumes that the uncertain data resides in the so-called uncertainty set. In addition, constraint violation cannot be allowed for any realization of data in the uncertainty set (Bram L. Gorissen and den Hertog, 2015). Therefore, for unknown probability distributions such as wind power data, robust optimization is the most suitable option between these approaches.

1.2 Problem statement

Renewable power capacity is set to expand worldwide by 50% between 2019 and 2024, led by solar photovoltaic. This increase of 1200 GW is equivalent to the total installed power capacity of the United States today (IEA, 2019). This implies that the conventional models for the operation of power systems have to be modified in order to include these new technologies; one of these classical models is the dispatch of hydrothermal systems, which is defined in (Christensen and El-Hawary, 1979) and in (Kothari and Dhillon, 2007) as the distribution of total generation requirements among all energy sources in the most optimal manner, taking into account the limitations of the system, so that an uninterrupted supply can be made available to the consumers.

This problem has different approaches which can be classified on the basis of the time horizon. In doing so, the economic dispatch is divided in long (2 months to several years), medium (1 week to 2 months) and short-term (1 day to 1 week)(J.Wood and F.Wollenberg, 1996)(Fuentes-Loyola and Quintana, 2003). These models are hierarchical since the long and medium term models give the final constraints for the short-term dispatch. Each of these models has a different source of complexity since the long and medium term are represented as a stochastic-linear model while the short-term hydrothermal coordination is usually a deterministic non-linear/non-convex problem (Kothari and Dhillon, 2007). Therefore, in the first and second cases, the problem is how to deal with the uncertainty taking into account a large number of scenarios, whereas in the last case, the problem is related with the high non-linearity/non-convexity of the model. Nevertheless, solar and wind energy introduce stochasticity to the short-term model making it even more complex. The main problem is therefore, how to deal with the non-linear/non-convex and stochastic nature of the short

term hydrothermal coordination.

In order to improve the accuracy and the convergence time of the algorithms used to solve this problem, methodologies that considers the non-convexity of the problem are required. In addition, it is necessary to develop tools that allow system operators make decisions, with an specific exactitude level, when they are dispatching wind and solar generators.

1.3 State of the Art

The short-term hydrothermal scheduling (STHS) is a classic problem in power system operation. That is why a large amount of research have been carried out in order to advance on the understanding and modeling of this problem. However, the typical configuration of the power system is changing due to the advent of new technologies such as renewable energy which requires new methodologies that consider thereof. Furthermore, its non-convex nature requires an accurate solving techniques that deals with its geometry.

In the very early years, deterministic optimization methods were widely used to solve the problem. Accordingly, several studies based on Lagrangian methodologies for solving the hydrothermal coordination problem were presented in (Slodoban Ruzic and Rajakovic, 1996), (Ruzic and Rajakovic, 1998), (Rodrigues and Edson L. da Silva, 2011) and (Fabricio Y.K. Takigawa and Rodrigues, 2012). The problem was also studied with Lagrangian relaxation and dynamic programming in (Md. Sayeed Salam and Hamdan, 1998) and (Md. Sayeed Salam and Hamdan, 1997). In (Houzhong Yan and Guan, 1993) the hydro sub-problem was formulated as a linear programming problem without accounting for the non-linear characteristics, while the thermal sub-problem was solved by applying a dynamic programming approach(Z. Yu and Smardo, 2000). In addition, a four-dimensional piecewise linear model was proposed in (Andre Luiz Diniz, 2008) where the water head was taken into account as a function of forebay and tailrace levels and spillage effects were considered. Otherwise, a parallel processing strategy was developed in (Tiago Norbiato Santos and Borges, 2017) to solve a multi-period problem in the context of multi-stage Benders decomposition.

Several mixed-integer linear programming formulations were presented in (Jinbao Jian and Yang, 2019), (Gil and Araya, 2016) and (Parrilla and Garcıa-Gonzalez, 2006). On the other hand, mixed-integer non-linear approach has also been used to face this problem. In (J.P.S. Catalao and Mendesb, 2010) hydroelectric power generation was considered as a non-linear function of water discharge and of the head, where the on-off behavior of the hydro plants were modeled by using integer variables, in order to avoid water discharges at forbidden areas. In (J.P.S. Catalao and c, 2011), Catalao proposes a mixed-integer non-linear approach to solve the short-term hydro scheduling problem in the

day-ahead electricity market, considering not only head-dependency, but also start/stop of units, discontinuous operating regions and discharge ramping constraints.

However, these methods did not deal with non-linearities of the problem in an accurate way. Therefore, several authors focused their research on coding the problem in such a way that heuristic techniques could be used. Thus, genetic algorithms (GA) have been widely used; the main idea of this kind of algorithms was to represent candidate solutions as individuals submitted to an evolutionary process. In (Amirarslan Haghrah and Seyedmonir, 2015), (Yong-Gang Wu and Wang, 2000),(Jarnail S. Dhillon and Kothary, 2011), (Sasikala and Ramaswamy, 2010), (Amjady and Nasiri-Rad, 2009),(Kumar and Naresh, 2007),(Chen and Chang, 1996), (E. Gil and Rudnick, 1264) and (Orero and Irving, 1998) GA were used, while (Nidul Sinha and Chattopadhyay, 2003), (Yongqiang Wang and Zhang, 2012) and (P. K. Hota and Chattopadhyay, 1999) developed optimization methodologies based on evolutionary process to find a good quality solution. Moreover, (Lakshminarasimman and Subramanian, 2006), (Manda and Chakraborty, 2008), (Sivasubramani and Swarup, 2011), (Basu, 2014) and (Youlin Lu and Zhang, 2010) introduced several differential algorithm which combine simple arithmetic operator with classic evolutionary operators, such as, mutation, crossover and selection in order to avoid prematuure convergence. Likewise, particle swarm optimization has also been used to solve this problem in (J. Zhang and Yue, 2012), (B. Yu and Wang, 2007), (Yuqiang Wua and Liu, 2019),(A.Rasoulzadeh-akhijahani and Mohammadi-ivatloo, 2015) and (P.K. Hota and Chakrabarti, 2009). This methodology simulates foraging process of birds in order to optimize process. Some others authors were inspired by the Newtonian laws of gravity and motion to carry out the short-term hydrothermal dispatch. Thus, Gravitational algorithms were proposed in (Chunlong Li and Peng Lu, 2015), (N. Gouthamkumar and Naresh, 2015), (Xiaotao Wu and Yuan, 2014) and (Gouthamkumar Nadakuditi and Naresh, 2016).

Quasi-opposition based learning was applied in (Basu, 2016) to enhance the capability of obtaining an optimal solution for STHS with consideration of valve point loading effect of thermal units, ramp rates of generation units, and power transmission losses. On the other hand, authors in (Nguyen and Vo, 2017) presented a modified cuckoo search algorithm for solving short-term hydrothermal scheduling. Other heuristic and metaheuristic techniques such as teaching learning based optimization, neural networks, clonal selection algorithm and Ant lion optimization have also been used in (Roy, 2013),(Yalcinoz and Short, 1998) (R. K. Swain and Chakrabarti, 2011) and (Hari Mohan Dubey and Panigrahi, 2016).

In the most recent years these techniques are still in use. Thereby, a quasi-reflected symbiotic organisms search was implemented for optimal scheduling of hydrothermal problems in (Sujoy Das and Chakraborty, 2018b). Shaikh S. Haroon investigated in (Haroon and Malik, 2017) a modified version of a new

nature inspired algorithm, called as evaporation rate–based water cycle algorithm, for the solution of STHS.

Due to the spreading of new technologies such as renewable energy, the classic STHS problem has had to be modified in order to consider the especial characteristics of these units. In doing so, several researchers have focused their studies on considering wind generation in the STHS. Thus, a genetic algorithm was proposed in (Yuan et al., 2015) where the model provided the reserve and compensation for the unplanned wind power output. This research utilized a metric based on the difference between the actual and planned output of wind power to calculate the additional system operation cost for wind uncertainty. Jianzhong Zhou proposed in (Jianzhong Zhou and Mo, 2016) an enhanced multi-objective bee colony optimization algorithm to solve the STHS including wind generation where the impact of wind power was considered by deriving a closed-form in terms of the incomplete gamma function. Similarly, in (Fang Chen and Lu, 2017), a gravitational algorithm is presented with a linearization of the relation between wind speed and wind power. In this way, the probability density function of wind power was obtained, which was used to calculate the coefficients cost of overestimating and underestimating wind generation. Said coefficient were used to calculate the optimal amount of power produced by wind units. In (Damodaran and Kumar, 2018) the same methodology was used to estimate the wind generation but, in this case, a modified particle swarm approach was utilized. Additionally, renewable units have high intermittency and volatility, which has restricted its penetration into power grid, that is why coordination scheduling of flexible resources and wind energy can be a interesting technique for promoting wind power utilization. In doing so, an improved multi-objective particle swarm optimization was proposed in (Yachao Zhang and An, 2018) in the interest of integrating large-scale electric vehicles with hydrothermal-wind multi objective scheduling. This algorithm also considered wind power cost by underestimating and overestimating cost functions in order to schedule wind generation.

When it comes to the integration of renewable technologies not only the technical aspects are important but also the economic ones. That is why (Beatriz P. Cotiaa and Dinizb, 2019) assessed some important economic issues that arise with increased wind power penetration in hydrothermal systems by using a mixed-Integer programming approach and where the results showed that restricting the injection of mandatory wind generation into the grid can reduce the total operation cost.

In addition, integration of both, solar and wind generation, to the traditional STHS problem has also been studied. In (Chaoshun Li and Chen, 2019) a hybrid grey wolf-multi-objective optimization algorithm was proposed by considering uncertainty of wind and solar generation under a scenarios approach, and creating clusters of unit status associated with a probability of occurrence. Ruey-Hsun Liang, went further in (Chen, 2016) by proposing a virus-evolutionary

differentiated-particle swarm optimization approach for short-term generation scheduling considering the change of atmospheric flow during the day and night, the uncertainties in the load demand, available water in the reservoir, wind speed, and radiation. Said uncertainties were faced by building a model with their density distribution functions. (Xuebin Wang and Wang, 2019) explored the relationship between the outflow of hydropower plants and coordinated effectiveness by setting different water availability scenario and proposing a coordinated operation model of power systems with hydrothermal-wind-photovoltaic power that considers the comprehensive utilization of reservoirs. Moreover, a complementary coordinated operation model of interconnected power systems, with hydrothermal-wind-photovoltaic plants, was proposed in (Xuebin Wang and Wang, 2018) to mitigate the curtailment problem of renewable energy by maximizing the new energy power generation and minimizing the thermal output fluctuation. This methodology considers the intersection of the maximum consumption capacity and the expected output of new energy power as the decision space to schedule wind and solar units. On the other hand, Sujoy Das proposed a probabilistic short-term hydrothermal-wind-photovoltaic scheduling based on the point estimate method in (Sujoy Das and Chakraborty, 2018a). Larger reviews about the optimization methods used to solve the STHS can be found in (Jiehong Kong and Fosso, 2020), (Farhat and El-Hawary, 2009) and (M. Nazari-Heris and Gharehpetian, 2017).

These heuristics and linearizations managed the non-linearity and noncovexity of the problem at the expense of a high computational cost and losing information. In addition, despite of its common use in power system applications, metaheuristic techniques have faced a lot of criticism such as lack of use on practical situations and lack of innovation. Moreover, its approach based on getting "a better solution" at expense of understanding the real optimization problem, has produced its rejection in the scientific community (Sorensen, 2015). That is why they are not suitable in the new context of the power systems operation where a high flexibility, better understanding of the problem, real time operation and high accuracy are required.

Convex approximation of the hydrothermal coordination problem is a relatively new subject. Some authors have tried to deal with the non-convexity of the problem by using different techniques. In (Fuentes-Loyola and Quintana, 2003) a semi-definite relaxation was proposed to face with the combinatorial characteristic of the medium term hydrothermal dispatch. Under other conditions, a semi-definite relaxation was presented in (Yunan Zhu and Yang, 2013) in order to deal with the non-convexity of the hydro power equation in a rigorous mathematical way. However, semidefinite programming has to deal with a large amount of spare matrix that implies a large computational burden.

On the other hand, Second-order cone optimization is a convex programming alternative which has been widely used in several electrical engineer problems such as designing even-order finite-impulse-response variable fractional-

delay digital filters (Deng, 2011), developing new control strategies (Jing Liu and Wong, 2003) and AC–DC power flow (Ye Zhou and Ghandhari, 2017) since SOC requires less computational effort. Nevertheless, to the best of the author knowledge, SOC programming has not been used to solve the STHS problem.

1.4 Contributions

The traditional STHS is a highly non-linear and complex problem which can be faced under two different approaches: on one hand, the exact model is considered and it is solved by an approximate method which does not guarantee a global optimum. On the other hand, an approximation of the model is carried out and then, an exact solution technique is used.

Using an exact solution technique implies several advantage such as high accuracy and fast convergence. Thus, an efficient methodology was established to solve a convex approximation of the original non-convex STHS model which always guarantees a global optimum of the approximated model and fast convergence. In addition, renewable generators were also considered modelling its stochastic behavior under a robust approach. Said approach was also used to model the stochastic behavior of the load. Furthermore, delays of flows through hydraulic chains and constraints that the grid imposes to generators were also evaluated.

As result of this research, a conference paper was presented in the 13th IEEE PowerTech 2019 in Milan, Italy.

1.5 Document organization

The rest of the document is organized as follows : Chapter 2 presents the mathematical models of generator units, as well as the DC powerflow and how to consider the grid and the renewable sources into the STHS. Next, in Chapter 3, some basic aspects of SOC programming are explained and a convex model for the STHS is proposed. In Chapter 4, the robust model that considers the stochasticity of load, wind units and solar power plants is developed. Chapters 5 and 6 present the results and the conclusions of the research. The test system used and all its parameters are presented in Appendix A; Appendix B explains some basic concepts of convex optimization. Finally, Appendix C presents the basic concepts of a probabilistic space.

Chapter 2

Deterministic Mathematical Model

This chapter presents the basic model of the system, starting from the model of each component. Then a non-linear programming problem is formulated and the convex and non-convex constrains are identified.

2.1 Modeling components

2.1.1 Thermal units

A large amount of generators in extant systems are of the fossil type (coal, oil or gas). This kind of technology takes advantages of the chemical energy stored in some fossil fuels by burning them in a boiler. In doing so, the chemical energy is converted into thermal energy which is transmitted to a fluid, usually water. The high pressure steam passes by a steam turbine which converts the kinetic and pressure energy of the steam into rotational kinetic energy. Since the electrical generator and the steam turbine are connected by a shaft, the rotational kinetic energy is turned into electrical energy which can be delivered to the grid as Figure 2.1 depicts. The electrical output of this set is connected, not only to

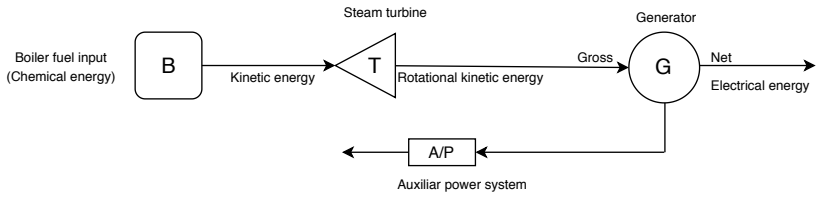

Figure 2.1: Boiler-turbine-generator unit (J.Wood and F.Wollenberg, 1996).

the electric network but also to the auxiliary power system in order to supply the electrical necessities of the power plant (J.Wood and F.Wollenberg, 1996).

In the STHS problem, the output power of these units is modeled as a variable which varies between a maximum value and a minimum value, as follows:

$$P_{Th_{min}} \leq P_{Th} \leq P_{Th_{max}} \tag{2.1}$$

On one hand, $P_{Th_{min}}$ is the minimum loading limit which depends on either uneconomical operation points or technically infeasible values. On the other hand, $P_{Th_{max}}$ is the maximum output limit given by the capacity of the group turbine-generator of by stability constraints (Kothari and Dhillon, 2007).

This technology has high operation costs since a large amount of fossil fuel is required to keep the plant operating. The curve that models the cost is approximated as a quadratic function of the active power generated (Figure 2.2).

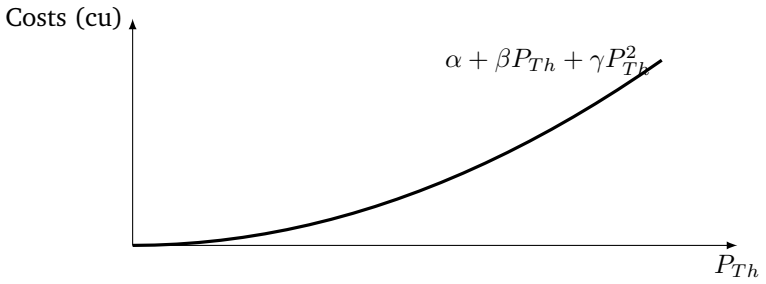

Figure 2.2: Cost function for thermal units. The function is convex if $\gamma \geq 0$

This curve can be obtained on the basis of the unit input-output characteristics or from the plant design engineers. It is normally function of unit design parameters such as initial steam conditions, stages of reheat and the reheat temperatures, condenser pressure and the complexity of the regenerative feed-water cycle (J.Wood and F.Wollenberg, 1996)(Christensen and El-Hawary, 1979). Therefore, the cost function for a single thermal power plant is:

$$\text{Cost} = \ \alpha + \beta P_{Th} + \gamma P_{Th}^2, \text{ with } \gamma \geq 0 \tag{2.2}$$

It is not difficult to see that the operation cost of an electrical system purely composed of thermal units is given by (2.3):

$$\sum_{i \in \Delta} (\alpha^i + \beta^i P_{Th}^i + \gamma^i (P_{Th}^i)^2), \text{ with } \gamma^i \geq 0 \tag{2.3}$$

where Δ is the set of all thermal units. In order to know the operating costs of the thermal generator set Δ, during the interval of time $S_T = (0, T)$ Equation (2.2) takes the form presented below:

$$\sum_{t\in\Omega}\sum_{i\in\Delta}(\alpha^i + \beta^i P_{Th}^{i,t} + \gamma^i (P_{Th}^{i,t})^2) \tag{2.4}$$

Equation (2.4) will be the objective function to minimize in this research. However, apart from the fuel cost, other objectives may be used, for example: minimum loss dispatch, best efficiency dispatch, replacement cost dispatch and emission dispatch. All of these objective functions are usually quadratic. Hence, the proposed model can be easily extended to these cases.

2.1.2 Hydro units

Conventional hydro plants are classified into run-of-river plants and storage plants. This type of plants consists of reservoirs which have large storage capacity. The volume of the reservoir depends on the water inflows, the spillage and the amount of water released to produce electricity during periods of high power requirements. During periods with low load requirements, potential energy is stored by filling the reservoir until its maximum limit, then water must be realized through the spillway, without producing electricity, in order to avoid that the water passes over the dam and produces damage in the civil structure. Figure 2.3 shows a basic configuration of a conventional hydro power plant.

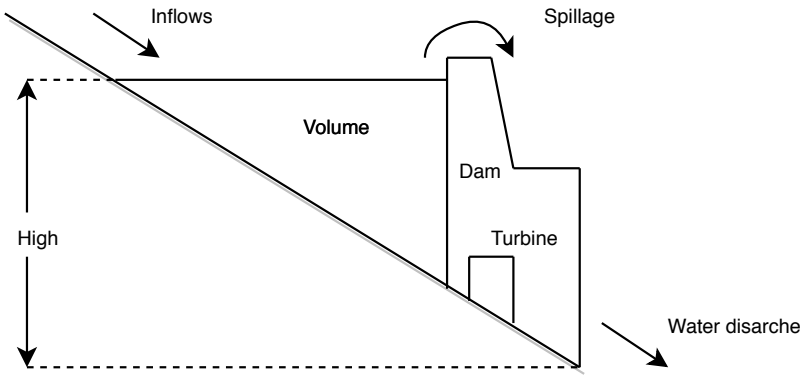

Figure 2.3: Basic configuration of a dam

The reason why electricity can be produced by using hydro power plants stems from the basic expression for potential energy:

$$E_p = mgh \tag{2.5}$$

.

It is not difficult to see that, if a mass of water m can be elevated to an altitude h, the mass of water is going to get a potential energy E_p. By deriving Equation (2.5) with respect to time, the hydro power takes the form of:

$$\frac{dE_p}{dt} = gh\frac{dm}{dt} = gh\rho\frac{dv}{dt} = gh\rho Q \tag{2.6}$$

The aforementioned equation represents the theoretical power produced by a hydro unit. However, real systems has intrinsic losses produced by the civil structures which are represented as a reduction of altitude h_L. In addition, electromechanical devices produce losses too which are considered by taking into account their efficiencies. In this way, and considering h_H as the headwater level, the power produced by a hydro unit is given as:

$$P_H = \eta\rho g(h_H - h_L)Q \tag{2.7}$$

Where Q is the water flow that passes by turbine, ρ represents the water density, g is the gravitational constant and η is the efficiency of the hydraulic machine.

However, Equation (2.7) does not represent the real behavior of the turbine, since it does not consider the changes that hydraulic head variation produces on the efficiency of the turbine. Therefore, a more accurate formulation is proposed in (Yunan Zhu and Yang, 2013). The power produced can be written as:

$$P_h(t) = C_1V(t)^2 + C_2Q(t)^2 + C_3V(t)Q(t) + C_4V(t) + C_5Q(t) + C_6 \tag{2.8}$$

Where coefficients C are the hydropower generation coefficients that depends on each unit, $V(t)$ is the volume of the reservoir and $Q(t)$ is the water discharges. Notices that this relation is non-linear in both, Q and V. It is important to mention that in this research, run-of-river plants were not considered since we are more interested on studying the non-convexity of the power produced by storage plants.

2.1.3 Wind units

Wind turbines are machines that convert the kinetic power of the air into electricity. The air passes through the blades which turns a shaft inside the nacelle. The shaft is connected to a gearbox with the purpose of increasing the rotational speed to reach the suitable speed for the electrical generator, which transforms the angular kinetic energy into electrical energy (Olimpo Anaya-Lara and Hughes, 2009).

The theoretical power produced by the air on an area Λ is given by (2.9), where ρ_{air} is the air density and v_w is the wind speed.

$$P_e = \frac{1}{2}\rho_{air}\Lambda v_w^3 \tag{2.9}$$

However, wind turbines are only capable to take a fraction of the power of the wind. The fraction of wind power that can be converted into electrical power is determined by the power coefficient C_p and is given by:

$$P_w = \frac{1}{2} C_P \rho_{air} \Lambda v_w^3 \tag{2.10}$$

The value of C_p depends on the inclination angle of the blades (β_p), called also pitch angle, and the ratio between the tangential speed of the tip of a blade and the actual speed of the wind (tip speed ratio λ_{tip}). So as to control the power produced, both, λ_{tip} and β_p must be modified.

Figure 2.4 depicts the wind turbine power behavior. From 0 to V_{cut-in} wind does not have enough energy to move the blades of the turbine. The interval between V_{cut-in} and V_{rated} represents how as the wind increases, the power increases in a cubical way until it reaches the rated power of the electrical generator. In this interval λ_{tip} is modified to obtain the maximum possible power. After that, wind gets V_{rated} and the pitch angle is changed to keep the power in its rated value in order to avoid damaging the electrical machine. The wind turbine can keep producing rated power until the wind speed is lower or equal to $V_{cut-out}$. At this moment mechanical devices have to stop the rotation of the blades and then the power produced is zero. Equation (2.11) represents the output power in per unit values (Basu, 2019).

$$P_{w_{P.U}}(v_w) = \begin{cases} 0 & v_w \leq v_{cut-in} \\ (\frac{v_w - v_{cut-in}}{v_{rated} - v_{cut-in}})^3 & v_{cut-in} \leq v_w \leq v_{rated} \\ 1 & v_{cut-in} \leq v_w \leq v_{cut-out} \\ 0 & v_w \geq v_{cut-out} \end{cases} \tag{2.11}$$

.

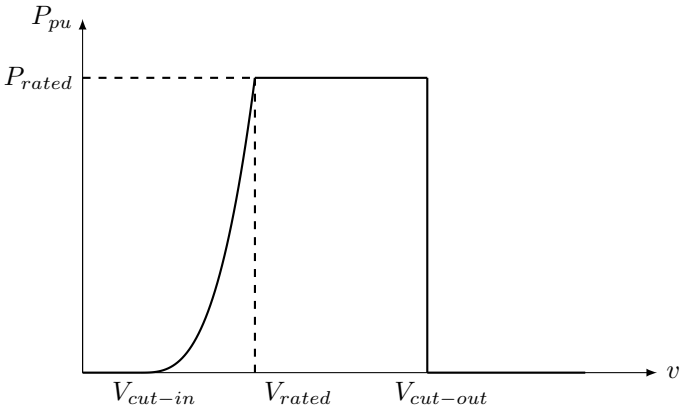

Figure 2.4: Wind power

Notice that wind is stochastic and hence, the outpout power is also stochastic.

2.1.4 Solar photovoltaic units

Photovoltaic units are power plants that works based on the capability of silicon materials to convert the energy contained in photons of light into an electrical current. A photon with wavelength and high energy can produce an electron in a photovoltaic material to escape from the atom that carries it. If an electric field is present, those electrons can be moved toward a metallic contact and an electric current appears(Masters, 2004).

The output power of this kind of unit is given by Equation (2.12) and depends on the solar irradiation ψ and the rated power of the photovoltaic system $P_{S_{rated}}$.

$$P_s = \frac{\psi \cdot P_{S_{rated}}}{1000} \tag{2.12}$$

The value 1000 comes from the nominal conditions that correspond to the panel tests and the units of ψ are W/m^2.

On the other hand, Equation (2.13) represents the capacity factor of a power plant which is defined as the ratio of the net electricity generated to the energy that could have been generated at continuous full-power operation during a considered interval of time.

$$C_{F_s} = \frac{E_s}{E_{rated}} = \frac{P_S \cdot\ t}{P_{S_{rated}} \cdot\ t} \tag{2.13}$$

If the capacity factor of the power plant C_{F_s} for a specific period t is known, the power produced by the unit can be calculated as:

$$P_S = C_{F_s} \cdot P_{S_{rated}} \tag{2.14}$$

In this research, the aforementioned equation was used to calculated the output power of the solar units since the available data corresponded to capacity factor data.

2.1.5 Classic short-therm hydrothermal dispatch model (Model I)

Short-term hydrothermal dispatch is an optimization problem which consists of minimizing the overall operation cost of thermal units by increasing the power that hydroelectrics produce in order to supply the load demand over a day or week, taking into account the physical and electrical constraints of the system (Kothari and Dhillon, 2007). The objective function and the constraints that model the problem are defined as follows:

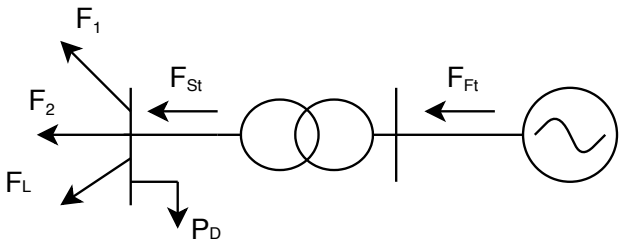

Figure 2.5: Flows through a node

- Cost function of the thermal plants

$$\text{Minimize} \sum_{t \in \Omega} \sum_{i \in \Delta} (\alpha^i + \beta^i \cdot P_{Th}^{i,t} + \gamma^i \cdot (P_{Th}^{i,t})^2) \tag{2.15}$$

The cost of power produced by the thermal units is a cuadratic function of the power produced, where the coefficients α, β and γ depend on the characteristics of each thermal power plant. The double sum in (2.15) stems from the cost of all thermal units operating during the interval of time studied. It is not difficult to see that the value α is related to the fixed operation costs.

- Active power balance

The law of conservation of energy states that the total energy of an isolated system remains constant. For a power system this principle means that the generated power, for all units of the system, must be iqual to the consumed power by the loads connected to said system at an interval of time t. For the sake of simplicity the losses were not considered and the balance equation can be written as:

$$\sum_{i \in \Delta} P_{Th}^{i,t} + \sum_{j \in S_H} P_H^{j,t} = P_D^t \tag{2.16}$$

From Figure 2.5 Equation (2.16) can be expressed, for the generator nodes as:

$$P_G^{k,t} = F_{Ft}^{k,t} \tag{2.17}$$

$$F_{Ft}^{k,t} = F_{St}^{k,t} \tag{2.18}$$

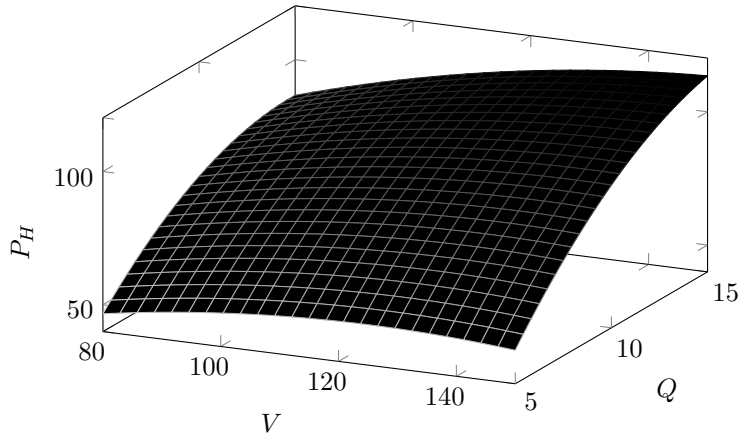

Figure 2.6: Quadratic function of Produced hydro power

$$F_{St}^{k,t} = \sum_{n \in N_k} F_L^{k,n,t} + P_D^{k,t} \tag{2.19}$$

Where $P_G^{k,t}$ is the power produced by generation units; $F_{Ft}^{k,t}$ and $F_{St}^{k,t}$ are the power flow through the primary and secondary of the transformer; $F_L^{k,n,t}$ are the flows through lines connected between the node k and the n node; finally $P_D^{k,t}$ represents the load.

- Hydroelectric generation

  The power produced by the hydro units is represented by a quadratic function of discharge and storage volume (see Figure 2.6). It is important to emphasize that this constraint is non-convex, since it is a not affine equality constraint, and it is going to determinate how difficult the problem is.

$$\begin{aligned} P_H^{j,t} = C_1^j \cdot V^{j,t^2} + C_2^j \cdot Q^{j,t^2} + C_3^j \cdot V^{j,t} \cdot Q^{j,t} \\ + C_4^j \cdot V^{j,t} + C_5^j \cdot Q^{j,t} + C_6^j \end{aligned} \tag{2.20}$$

- Continuity equation for the hydro reservoir network

  The volume of reservoir j at moment t is determined by: the volume that used to be at the moment $t-1$, the natural inflows of the reservoir, the water and the spillage released, and the water and the spillage that come from upper reservoirs. From figure 2.7, it is not difficult to see that the water that comes from an upper reservoir to a lower reservoir does not arrive immediately to the lower reservoir. The time that said mass

of water takes to move between reservoirs is called delay, and must be considered in order to accurately operate the hydro chains. This delay is represented by τ and it is different for each connection between reservoirs. On the other hand, it is important to highlight that the evaporation was not considered in this research.

$$V^{j,t} = V^{j,t-1} + I^{j,t} - Q^{j,t} - S^{j,t} + \sum_{\pi \in S_{\Omega j}} (Q^{\pi,t-\tau} + S^{\pi,t-\tau}) \tag{2.21}$$

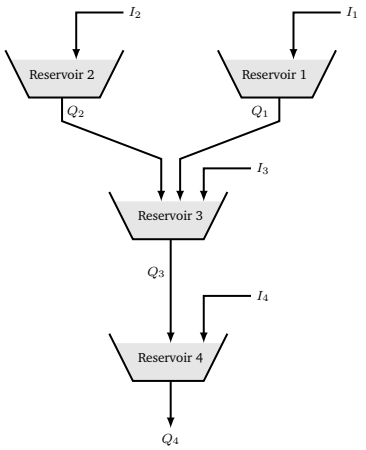

Figure 2.7: Hydraulic system test network. Data for this test system is available in (Orero and Irving, 1998)

- Initial and final reservoir storage volumes

$$V^{j,0} = V^{j}_{ini} \tag{2.22}$$

$$V^{j,T} = V^{j}_{end} \tag{2.23}$$

- Physical limitations on reservoir storage volumes, discharge rates and power generation.

$$V^{j}_{min} \leq V^{j,t} \leq V^{j}_{max} \tag{2.24}$$

$$Q^{j}_{min} \leq Q^{j,t} \leq Q^{j}_{max} \tag{2.25}$$

$$P^{i}_{Th_{min}} \leq P^{i,t}_{Th} \leq P^{i}_{Th_{max}} \tag{2.26}$$

$$P_{H^j_{min}} \leq P^{j,t}_H \leq P_{H^j_{max}} \tag{2.27}$$

$$S^j_{min} \leq S^{j,t} \leq S^j_{max} \tag{2.28}$$

It is important to emphasize that the aforementioned constraints must be satisfied at any moment t.

2.1.6 DC powerflow

Notice that Equations (2.17), (2.18) and (2.19) imply that the power flows through lines must be known. Different types of methodologies has been used to solve the power flow problem, must of them require to know the electrical characteristics of the grid, angles and voltages of each node. However, those methodologies have large computational burden. That is why DC power flow is commonly used to solve and simplify this problem when it is working with high voltage levels. Said method assumes that the voltages are sustained at 1 per unit, which is a valid assumption in electrical power systems, where control methodologies try to keep the voltages close to this value. In addition, each line is represented by its series reactance (Grainger and Jr., 1994). In this way, the per unit power flow from node k to node n in a line with series reactance $X_{kn_{P.U}}$ with angular difference $\theta_{k,n}$ is given by:

$$P_{kn_{P.U}} = \frac{sin(\theta_{kn})}{X_{kn_{P.U}}} \tag{2.29}$$

By considering $sin(\theta_{kn}) \simeq \theta_{kn}$, the aforementioned Equation takes the form of Grainger and Jr. (1994):

$$P_{kn_{P.U}} = \frac{\theta_{kn}}{X_{kn_{P.U}}} \tag{2.30}$$

On the other hand, the injected power at each node can be calculated as:

$$[P_{P.U}] = [B_{P.U}][\theta] \tag{2.31}$$

Where $[P_{P.U}]$ is the vector of active injected powers; $[B_{P.U}]$ is the nodal admitance matrix and [θ] is the vector of angles between adjacent nodes.

By considering that the injected power at node k is given by the difference between the generated power and load connected to the aforementioned node, Equation (2.31) takes the following form:

$$[P_{G_{P.U}}] - [P_{D_{P.U}}] = [B_{P.U}][\theta] \tag{2.32}$$

From Figure 2.5 it is easy to see that the power injected at node k at moment t must be equal to the flows through the lines connected to this node. Said relation is given as follows:

$$P_{G_{P.U}}^{k,t} - P_{D_{P.U}}^{k,t} = \sum_{n \in N_k} F_{L_{P.U}}^{k,n,t} \tag{2.33}$$

Where N_k is the set of nodes connected to the node k.

The data of the grid used in this research can be found in Appendix A.

2.1.7 STHS with wind and solar resources

In order to include wind and solar generators in the traditional model the equations of flow balance, for the nodes where these types of generators exist, are modeled as:

$$P_{G_{P.U}}^{k,t} = P_{w_{P.U}}^{k,t} \; for \; k = e \tag{2.34}$$

$$P_{G_{P.U}}^{k,t} = P_{s_{P.U}}^{k,t} \; for \; k = u \tag{2.35}$$

Where P_w and P_s are given by (2.11) and (2.14). However, these equations do not consider the stochasticity of the renewable resources.

2.2 Convex qualification and challenge of the model

Notice that the objective function (2.15) is a quadratic convex function; Equations (2.16)-(2.19), (2.21)-(2.23) and (2.30)-(2.33) shape affine spaces; Equations (2.24)-(2.28) and (2.34)-(2.35) are box constraints. Finally, Equation (2.20) is not affine which makes the model non-convex.

The main challenges of this model lie on the stochastic nature of wind and solar generation and its non-linear and non-convex characteristics. Therefore, convex relaxations, to mention second-order cone relaxation, is a tool that helps to deal with the non-convexity of quadratic non-convex constraints. This will be presented in the next chapter.

In order to deal with the inherent stochasticity of renewable sources, a robust optimization approach which allows to satisfy the probabilistic constraints, is considered in this research as presented in Chapter 4.

Chapter 3

Second-order cone programming for the STHS

This chapter shows the convexification of the short-term hydrothermal scheduling problem, using second order cone programming. The main characteristics of these type of optimization models are also presented.

3.1 The second order cone

A cone is a subset of a set ξ over a linear space such as, for each $Y \in \xi$ and a positive scalar number $\wp$, we have $\wp Y \in \xi$. There are several kind of cones, however we are interested in the second order cone, more especefically in the programming problems associated with this geometry.

Second-order cone programming problems are convex optimization problem of the form minimizing a linear function subject to affine linear constraints and cartesian product of second-order cone constrains. Moreover, convex quadratic problems and quadratically constrained convex quadratic problems (QCQP) can be formulated as SOC problems. The general structure of a second-order cone problems is presented below:

$$\text{minimize } f^{\top}Y \tag{3.1}$$

$$\text{subject to } \|A_iY + b_i\|_2 \leq c_iY + d_i,\ i = 1, ..., m \tag{3.2}$$

$$UY = \varrho \tag{3.3}$$

Notice that constraints such as Equation (3.2) define a cone of the form depicted in Figure 3.1. It is not difficult to see thereof cone holds the convexity criteria explained in subsection B.2 of Appendix B. Moreover, primal or dual interior point methods developed for linear programming can be extended in

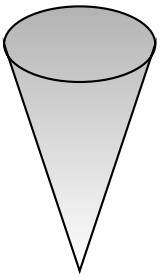

Figure 3.1: Second-order cone

a word-for-word fashion to SOC. In this way, there are several software package available to handle SOC programming problems, namely: Gurobi, Sedumi, Mosek, etc. (Alizadeh and Goldfarb, 2003).

3.2 Quadratically constrainted quadratic programming problems

A convex optimization problem can be considered as quadratically constrainted quadratic programming problem (QCQP) if the objective function and the associated constraints can be defined as follows:

$$\text{minimize } Y^\top P_0 Y + 2q_0^\top Y + r_0 \tag{3.4}$$

$$\text{subject to } Y^\top P_i Y + 2q_i^\top Y + ri \leq 0 \tag{3.5}$$

In this case, a convex quadratic function is minimized over a feasible region that is the intersection of ellipsoids (Boyd and Vndenberghe, 2009).

Problems of the form of QCQP can be rewritten as SOC by using the concept of epigraph (see (Alizadeh and Goldfarb, 2003)) if and only if the matrix P_0 and P_i admit cholesky decomposition, that is to say $P_i = (P_i^{-1/2})^\top \cdot (P_i^{1/2})$, which implies that both, P_0 and P_i must be positive semidefinite matrix.

The general structure of a QCQP problem rewritten as a SOC problem takes the form of:

$$\text{minimize } z \tag{3.6}$$

$$\text{subject to } \left\| P_0^{1/2} Y + P_0^{-1/2} q_0 \right\| \leq z \tag{3.7}$$

$$\left\| P_i^{1/2} Y + P_i^{-1/2} q_0 \right\|_2 \leq (q_i^\top P_i^{-1} q_i - r_i)^{1/2} \tag{3.8}$$

$$UY = \varrho \tag{3.9}$$

where, for a given matrix P, it is defined $P^{1/2}$ as the matrix that is generated from the Cholesky decomposition, such as $P = (P^{1/2})^\top \cdot (P^{1/2})$. Likewise, $P^{-1/2}$ is defined as $P^{-1/2} = ((P^{1/2})^{-1})^\top$ such as $(P^{-1/2})^\top \cdot (P^{1/2}) = I$.

On the other hand, equations of the form of (3.5) and (3.8) can also be rewritten as:

$$\left\| \begin{pmatrix} \frac{1+2q_i^\top Y + r_i}{2} \\ P_i^{1/2} Y \end{pmatrix} \right\|_2 \leq \frac{1 - 2q_i^\top Y - r_i}{2} \tag{3.10}$$

Next section explains how Equation (3.10) is deduced.

3.3 Quadratically constraint rewritten as second-order cone constraint

An equation given as Equation (3.11)

$$Y^\top \cdot (P_i^{1/2})^\top \cdot (P_i^{1/2}) \cdot Y + 2q_i^\top Y + r_i \leq 0 \tag{3.11}$$

can be rewritten as SOC constraint of the form of Equation (3.12)

$$\left\| \begin{pmatrix} \frac{1+2q_i^\top Y + r_i}{2} \\ (P_i^{1/2}) Y \end{pmatrix} \right\| \leq \frac{1 - 2q_i^\top Y - r_i}{2} \tag{3.12}$$

In order to prove this, let us calculate the Euclidian norm of the vector to the right side of Equation (3.12), and then expanding the expression as follows:

$$\sqrt{\frac{(1+2q_i^\top Y + r_i)}{2} \cdot \frac{(1+2q_i^\top Y + r_i)}{2} + ((P_i^{1/2})Y)^\top \cdot ((P_i^{1/2})Y)} \leq \frac{1 - 2q_i^\top Y - r_i}{2} \tag{3.13}$$

$$\frac{1}{4} + \frac{(2q_i^\top Y)^2}{4} + \frac{r_i^2}{4} + \frac{2q_i^\top Y}{2} + \frac{r_i}{2} + \frac{r_i 2q_i^\top Y}{2} + ((P_i^{1/2})Y)^\top \cdot ((P_i^{1/2})Y) \leq \frac{(1 - 2q_i^\top Y - r_i)^2}{4} \tag{3.14}$$

$$\begin{aligned}\frac{1}{4}+\frac{(2q_i^\top Y)^2}{4}+\frac{r_i^2}{4}+\frac{2q_i^\top Y}{2}+\frac{r_i}{2}+\frac{r_i 2q_i^\top Y}{2}+Y^\top(P_i^{1/2})^\top\cdot(P_i^{1/2})Y \\ \leq \frac{1}{4}+\frac{(2q_i^\top Y)^2}{4}+\frac{r_i^2}{4}-\frac{2q_i^\top Y}{2}-\frac{r_i}{2}+\frac{r_i 2q_i^\top Y}{2}\end{aligned} \tag{3.15}$$

$$Y^\top(P_i^{1/2})^\top(P_i^{1/2})Y+2q_i^\top Y+r_i\leq 0 \tag{3.16}$$

3.4 Convex approximation for the STHS model

In order to obtain a convex relaxation of the Equation 2.20 let us approximate this Equation as follows:

$$\begin{aligned}P_H^{j,t}\leq C_1^j V^{j,t^2}+C_2^j Q^{j,t^2}+C_3^j V^{j,t}.Q^{j,t} \\ +C_4^j V^{j,t}+C_5^j Q^{j,t}+C_6^j\end{aligned} \tag{3.17}$$

The aforementioned approximation can be carried out due to the the fact that the objective function to minimize is the production cost of thermal generators and the generation cost of hydro units is zero. Consequently, the optimization process tends to use as much hydropower as possible; therefore, setting a top limit on this variable is an equivalent approximation of the Equation (2.20). Additionally, Equation (3.17) can be rewritten as presented below:

$$\begin{aligned}P_{Th}^{j,t}\leq \begin{pmatrix}Q^{j,t} & V^{j,t}\end{pmatrix}\cdot\begin{pmatrix}C_1^j & \frac{C_3}{2}^j \\ \frac{C_3}{2}^j & C_2^j\end{pmatrix}\cdot\begin{pmatrix}Q^{j,t}\\ V^{j,t}\end{pmatrix} \\ +\begin{pmatrix}C_4^j\\ C_5^j\end{pmatrix}\cdot\begin{pmatrix}Q^{j,t}\\ V^{j,t}\end{pmatrix}+C_6^j\end{aligned} \tag{3.18}$$

Where the matrix composed by the elements C_1^j, C_2^j and $\frac{C_3}{2}^j$ in Equation (3.18) is definite positive for all j, which implies that the non-convex equation of produced power by hydro unit can be approximated as a quadratic constraint. Moreover, according to what was explained in Sections 3.2 and 3.3, hydropower equation can be rewritten as follows:

$$\begin{aligned}-\begin{pmatrix}Q^{j,t} & V^{j,t}\end{pmatrix}\cdot\begin{pmatrix}C_1^j & \frac{C_3}{2}^j \\ \frac{C_3}{2}^j & C_2^j\end{pmatrix}\cdot\begin{pmatrix}Q^{j,t}\\ V^{j,t}\end{pmatrix} \\ -\begin{pmatrix}C_4^j\\ C_5^j\end{pmatrix}\begin{pmatrix}Q^{j,t}\\ V^{j,t}\end{pmatrix}-C_6^j+P_{Th}^{j,t}\leq 0\end{aligned} \tag{3.19}$$

It is not difficult to see that Equation (3.19) takes the form of a SOC constraint as follows:

$$\left\| \begin{pmatrix} \frac{1-\binom{C_4^j}{C_5^j}\binom{Q^{j,t}}{V^{j,t}}-C_6^j+P_H^{j,t}}{2} \\ \begin{pmatrix} -C_1^j & \frac{-C_3{}^j}{2} \\ \frac{-C_3{}^j}{2} & -C_2^j \end{pmatrix}^{\frac{1}{2}} \begin{pmatrix} Q^{j,t} \\ V^{j,t} \end{pmatrix} \end{pmatrix} \right\|_2 \leq \frac{1+\binom{C_4^j}{C_5^j}\binom{Q^{j,t}}{V^{j,t}}+C_6^j-P_H^{j,t}}{2} \quad (3.20)$$

For sake of completeness, let us define an auxiliary variable $\mathfrak{U}$ such as:

$$\mathfrak{U} = \frac{1+\binom{C_4^j}{C_5^j}\binom{Q^{j,t}}{V^{j,t}}+C_6^j-P_H^{j,t}}{2} \quad (3.21)$$

Hence, Equation 3.20 can be rewriting as follows:

$$\left\| \begin{pmatrix} \frac{1-\binom{C_4^j}{C_5^j}\binom{Q^{j,t}}{V^{j,t}}-C_6^j+P_H^{j,t}}{2} \\ \begin{pmatrix} -C_1^j & \frac{-C_3{}^j}{2} \\ \frac{-C_3{}^j}{2} & -C_2^j \end{pmatrix}^{\frac{1}{2}} \begin{pmatrix} Q^{j,t} \\ V^{j,t} \end{pmatrix} \end{pmatrix} \right\|_2 \leq \mathfrak{U} \quad (3.22)$$

3.5 Convex model of STHS (Model II)

By considering the relaxation proposed in section 3.4, the following STHS model is proposed:

$$\text{Minimize } z \quad (3.23)$$

subject to:

- Cost function of the thermal plants

$$\sum_{t\in\Omega}\sum_{i\in\Delta}\left\|(\gamma^i)^{1/2}P_{Th}^{i,t}+(\gamma^i)^{1/2}\frac{\beta^i}{2}\right\| \leq z \quad (3.24)$$

- Active power balance

$$\sum_{i\in\Delta}P_{Th}^{i,t}+\sum_{j\in S_H}P_H^{j,t}=P_D^t \quad (3.25)$$

- Hydroelectric generation

$$\left\| \begin{pmatrix} \frac{1-\begin{pmatrix} C_4^j \\ C_5^j \end{pmatrix} \begin{pmatrix} Q^{j,t} \\ V^{j,t} \end{pmatrix} - C_6^j + P_H^{j,t}}{2} \\ \begin{pmatrix} -C_1^j & \frac{-C_3{}^j}{2} \\ \frac{-C_3{}^j}{2} & -C_2^j \end{pmatrix}^{\frac{1}{2}} \begin{pmatrix} Q^{j,t} \\ V^{j,t} \end{pmatrix} \end{pmatrix} \right\|_2 \leq \mathfrak{U} \tag{3.26}$$

  Where the value of $\mathfrak{U}$ is given by Equation 3.21.

- Continuity equation for the hydro reservoir network

$$\begin{aligned} V^{j,t} = V^{j,t-1} + I^{j,t} - Q^{j,t} - S^{j,t} \\ + \sum_{\pi \in S_{\Omega^j}} (Q^{\pi,t-\tau} + S^{\pi,t-\tau}) \end{aligned} \tag{3.27}$$

- Initial and final reservoir storage volumes

$$V^{j,0} = V_{ini}^j \tag{3.28}$$

$$V^{j,T} = V_{end}^j \tag{3.29}$$

- Physical limitations on reservoir storage volumes, discharge rates and power generation.

$$V_{min}^j \leq V^{j,t} \leq V_{max}^j \tag{3.30}$$

$$Q_{min}^j \leq Q^{j,t} \leq Q_{max}^j \tag{3.31}$$

$$P_{Th_{min}}^i \leq P_{Th}^{i,t} \leq P_{Th_{max}}^i \tag{3.32}$$

$$P_{H_{min}^j} \leq P_H^{j,t} \leq P_{H_{max}^j} \tag{3.33}$$

$$S_{min}^j \leq S^{j,t} \leq S_{max}^j \tag{3.34}$$

3.6 Convex model of STHS considering the grid (Model III)

As it was said in section 2.1.6, the grid imposes constraints to the generators. Power flow constraints are considered into the short-term dispatch as:

$$P_{G_{P.U}}^{k,t} - P_{D_{P.U}}^{k,t} = \sum_{n \in N_k} F_{L_{P.U}}^{k,n,t} \tag{3.35}$$

$$F_{L_{P.U}}^{k,n,t} = \frac{\theta^{k,t} - \theta^{n,t}}{X_{k,n}} \tag{3.36}$$

$$[P_{G_{PU}}]^t - [P_{D_{PU}}]^t = [B_{PU}][\theta]^t \tag{3.37}$$

It is important to consider that angular differences greater than $\frac{\pi}{2}$ can result in stability issues (Padiyar, 2008). Thus, the angle constraint is written as follows:

$$-\frac{\pi}{2} \leq \theta^{k,n,t} \leq \frac{\pi}{2} \tag{3.38}$$

In addition, the transmission lines have a maximum power conduction capacity which depends on several aspects such as temperature, voltage stability and angle stability. In doing so, from Equations (2.29) and (3.38), the maximum capability of the line can be calculated as Equation (3.39) if the power transfer limit is set by the stability angle (Jan Machowski, 2008).

$$F_{L_{max\ P.U}}^{k,n} = \frac{sin(\theta_{kn})_{max}}{X_{kn_{P.U}}} = \frac{sin(\frac{\pi}{2})}{X_{kn_{P.U}}} = \frac{1}{X_{kn_{P.U}}} \tag{3.39}$$

Similarly, the minimum capability of the line can be considered as:

$$F_{L_{min\ P.U}}^{k,n} = \frac{sin(\theta_{kn})_{min}}{X_{kn_{P.U}}} = \frac{sin(-\frac{\pi}{2})}{X_{kn_{P.U}}} = \frac{-1}{X_{kn_{P.U}}} \tag{3.40}$$

Thus, and by considering a proportion of 1 to 6.5 between the thermal capacity and the stability capacity of the line, the maximum and minimum power can be considered as Equation (3.41) (kundur, 1994).

$$F_{L_{Tmin\ P.U}}^{k,n} \leq F_{L_{P.U}}^{k,n,t} \leq F_{L_{Tmax\ P.U}}^{k,n} \tag{3.41}$$

Notice that the superscript t in Equation (3.37) implies that the DC power flow must be run for each interval of time t. In addition, it is important to highlight that Equations (3.38) and (3.41) are a box constraints which match with convexity criteria.

By considering Equations (3.35), (3.37),(3.38) and (3.41) the STHS model that considers the grids is described as follows:

$$\text{Minimize } z \tag{3.42}$$

Subject to:

- Cost function of the thermal plants

$$\sum_{t\in\Omega}\sum_{i\in\Delta}\left\|(\gamma^i)^{1/2}P_{base}P^{i,t}_{Th_{P.U}}+(\gamma^i)^{1/2}\frac{\beta^i}{2}\right\|\leq z \tag{3.43}$$

  Notice that this model has to be treated in values in per unit (P.U). Otherwise, DC power flow could not be used.

- Active power balance

$$P^{k,t}_{D_{P.U}}=F^{k,t}_{St_{P.U}}-\sum_{n\in N_k}F^{k,n,t}_{L_{P.U}} \tag{3.44}$$

$$P^{k,t}_{G_{P.U}}=F^{k,t}_{Ft_{P.U}} \tag{3.45}$$

$$F^{k,t}_{Ft_{P.U}}=F^{k,t}_{St_{P.U}} \tag{3.46}$$

- Power flow constraints

$$[P_{G_{PU}}]^t-[P_{D_{PU}}]^t=[B_{PU}][\theta]^t \tag{3.47}$$

$$F^{k,n,t}_{L_{P.U}}=\frac{\theta^{k,t}-\theta^{n,t}}{X_{k,n}} \tag{3.48}$$

$$F^{k,n}_{L_{Tmin\ P.U}}\leq F^{k,n,t}_{L_{P.U}}\leq F^{k,n}_{L_{Tmax\ P.U}} \tag{3.49}$$

$$-\frac{\pi}{2}\leq\theta^{k,n,t}\leq\frac{\pi}{2} \tag{3.50}$$

- Hydroelectric generation

$$\left\|\begin{pmatrix}\frac{1-\begin{pmatrix}C^j_{4_{P.U}}\\C^j_{5_{p.u}}\end{pmatrix}\begin{pmatrix}Q^{j,t}_{P.U}\\V^{j,t}_{P.U}\end{pmatrix}-C^j_{6_{p.u}}+P^{j,t}_{H_{P.U}}}{2}\\ \begin{pmatrix}-C^j_{1_{P.U}} & \frac{-C_{3_{P.U}}{}^j}{2}\\ \frac{-C_{3_{P.U}}{}^j}{2} & -C^j_{2_{P.U}}\end{pmatrix}^{\frac{1}{2}}\begin{pmatrix}Q^{j,t}_{P.U}\\V^{j,t}_{P.U}\end{pmatrix}\end{pmatrix}\right\|_2\leq\mathfrak{U}_{P.U} \tag{3.51}$$

  Where the value of $\mathfrak{U}$ is given by Equation 3.21.

- Continuity equation for the hydro reservoir network

$$V_{P.U}^{j,t} = V_{P.U}^{j,t-1} + I_{P.U}^{j,t} - Q_{P.U}^{j,t} - S_{P.U}^{j,t} + \sum_{\pi \in S_{\Omega j}} (Q_{P.U}^{\pi,t-\tau} + S_{P.U}^{\pi,t-\tau}) \tag{3.52}$$

- Initial and final reservoir storage volumes

$$V_{P.U}^{j,0} = V_{ini_{P.U}}^{j} \tag{3.53}$$

$$V_{P.U}^{j,T} = V_{end_{P.U}}^{j} \tag{3.54}$$

- Physical limitations on reservoir storage volumes, discharge rates, power generation, line capacities and angles.

$$V_{min_{P.U}}^{j} \leq V_{P.U}^{j,t} \leq V_{max_{P.U}}^{j} \tag{3.55}$$

$$Q_{min_{P.U}}^{j} \leq Q_{P.U}^{j,t} \leq Q_{max_{P.U}}^{j} \tag{3.56}$$

$$P_{Th_{min_{P.U}}}^{i} \leq P_{Th_{P.U}}^{i,t} \leq P_{Th_{max_{P.U}}}^{i} \tag{3.57}$$

$$P_{H_{min_{P.U}}}^{j} \leq P_{H_{P.U}}^{j,t} \leq P_{H_{max_{P.U}}}^{j} \tag{3.58}$$

$$S_{min_{P.U}}^{j} \leq S_{P.U}^{j,t} \leq S_{max_{P.U}}^{j} \tag{3.59}$$

- Generated power

  The produced power at a node k depends on the type of the unit connected to this node. For the traditional STHS there are two types of generation: hydro and thermal. In this way, the power generations at node k is given as:

$$P_{G_{P.U}}^{k,t} = P_{Th_{P.U}}^{i,t} \; for \; k = i \tag{3.60}$$

$$P_{G_{P.U}}^{k,t} = P_{H_{P.U}}^{j,t} \; for \; k = j \tag{3.61}$$

3.7 Deterministic convex model of STHS considering the grid and renewable sources (Model IV)

This subsection presents a convex model for STHS considering renewable sources and the grid. It is important to highlight that the stochasticity of renewable sources is not considered. In this case, values of wind speed and solar irradiation are considered known values. Thus, the model is present as follows:

$$\text{Minimize } z \tag{3.62}$$

Subject to:

- Cost function of the thermal plants

$$\sum_{t\in\Omega}\sum_{i\in\Delta}\left\|(\gamma^i)^{1/2}P_{base}P^{i,t}_{Th_{P.U}}+(\gamma^i)^{1/2}\frac{\beta^i}{2}\right\|\leq z \tag{3.63}$$

- Active power balance

$$P^{k,t}_{D_{P.U}}=F^{k,t}_{St_{P.U}}-\sum_{n\in N_k}F^{k,n,t}_{L_{P.U}} \tag{3.64}$$

$$P^{k,t}_{G_{P.U}}=F^{k,t}_{Ft_{P.U}} \tag{3.65}$$

$$F^{k,t}_{Ft_{P.U}}=F^{k,t}_{St_{P.U}} \tag{3.66}$$

- Power flow constraints

$$[P_{G_{PU}}]^t-[P_{D_{PU}}]^t=[B_{PU}][\theta]^t \tag{3.67}$$

$$F^{k,n,t}_{L_{P.U}}=\frac{\theta^{k,t}-\theta^{n,t}}{X_{k,n}} \tag{3.68}$$

$$F^{k,n}_{L_{Tmin\ P.U}}\leq F^{k,n,t}_{L_{P.U}}\leq F^{k,n}_{L_{Tmax\ P.U}} \tag{3.69}$$

$$-\frac{\pi}{2}\leq\theta^{k,n,t}\leq\frac{\pi}{2} \tag{3.70}$$

- Hydroelectric generation

$$\left\|\begin{pmatrix}\frac{1-\begin{pmatrix}C^j_{4_{P.U}}\\C^j_{5_{p.u}}\end{pmatrix}\begin{pmatrix}Q^{j,t}_{P.U}\\V^{j,t}_{P.U}\end{pmatrix}-C^j_{6_{p.u}}+P^{j,t}_{H_{P.U}}}{2}\\ \begin{pmatrix}-C^j_{1_{P.U}} & \frac{-C_{3_{P.U}}{}^j}{2}\\ \frac{-C_{3_{P.U}}{}^j}{2} & -C^j_{2_{P.U}}\end{pmatrix}^{\frac{1}{2}}\begin{pmatrix}Q^{j,t}_{P.U}\\V^{j,t}_{P.U}\end{pmatrix}\end{pmatrix}\right\|_2\leq\mathfrak{U}_{P.U} \tag{3.71}$$

Where the value of $\mathfrak{U}$ is given by Equation 3.21.

- Continuity equation for the hydro reservoir network

$$V_{P.U}^{j,t} = V_{P.U}^{j,t-1} + I_{P.U}^{j,t} - Q_{P.U}^{j,t} - S_{P.U}^{j,t} + \sum_{\pi \in S_{\Omega j}} (Q_{P.U}^{\pi,t-\tau} + S_{P.U}^{\pi,t-\tau}) \tag{3.72}$$

- Initial and final reservoir storage volumes

$$V_{P.U}^{j,0} = V_{ini_{P.U}}^{j} \tag{3.73}$$

$$V_{P.U}^{j,T} = V_{end_{P.U}}^{j} \tag{3.74}$$

- Physical limitations on reservoir storage volumes, discharge rates, power generation, line capacities and angles.

$$V_{min_{P.U}}^{j} \leq V_{P.U}^{j,t} \leq V_{max_{P.U}}^{j} \tag{3.75}$$

$$Q_{min_{P.U}}^{j} \leq Q_{P.U}^{j,t} \leq Q_{max_{P.U}}^{j} \tag{3.76}$$

$$P_{Th_{min_{P.U}}}^{i} \leq P_{Th_{P.U}}^{i,t} \leq P_{Th_{max_{P.U}}}^{i} \tag{3.77}$$

$$P_{H_{min_{P.U}}}^{j} \leq P_{H_{P.U}}^{j,t} \leq P_{H_{max_{P.U}}}^{j} \tag{3.78}$$

$$S_{min_{P.U}}^{j} \leq S_{P.U}^{j,t} \leq S_{max_{P.U}}^{j} \tag{3.79}$$

- Wind generation

$$P_{w_{P.U}}^{e,t} = \begin{cases} 0 & v_w^{e,t} \leq v_{cut-in} \\ (\frac{v_w^{e,t} - v_{cut-in}}{v_{rated} - v_{cut-in}})^3 & v_{cut-in} \leq v_w^{e,t} \leq v_{rated} \\ 1 & v_{cut-in} \leq v_w^{e,t} \leq v_{cut-out} \\ 0 & v_w^{e,t} \geq v_{cut-out} \end{cases} \tag{3.80}$$

.

- Photovoltaic genaration

$$P_{S_{P.U}}^{u,t} = C_{F_s}^{u,t} \, P_{S_{rated\ P.U}}^{u} \tag{3.81}$$

- Generated power

$$P_{G_{P.U}}^{k,t} = P_{Th_{P.U}}^{i,t} \; for \; k = i \tag{3.82}$$

$$P_{G_{P.U}}^{k,t} = P_{H_{P.U}}^{j,t} \; for \; k = j \tag{3.83}$$

$$P_{G_{P.U}}^{k,t} = P_{w_{P.U}}^{e,t} \; for \; k = e \tag{3.84}$$

$$P_{G_{P.U}}^{k,t} = P_{S_{P.U}}^{u,t} \; for \; k = u \tag{3.85}$$

Notice that the components on the vector $[P_{G_{PU}}]^t$ depends of the kind of generator that is connected to the node, that is why it is necessary to specify what kind of generator we have in each node. Additionally, Equations 3.84 and 3.85 are used to calculate the power produced by these units when specific data are given.

Chapter 4

Robust model

Wind speed and solar irradiation are variables that cannot be predicted with exactitude. That implies that the optimization problems that deal with these variables, must consider their stochastic characteristics. Several approaches have been used when it comes to working with stochastic elements, stochastic optimization and robust optimization are some of them.

Even though both, stochastic optimization (SO) and robust optimization (RO), face optimization problems with random variables, they do it in different ways that differ considerably. Thus, in SO, these random data obey a known in advance probability distribution and therefore a way to calculate said probability distribution is required. On the other hand, in RO, it is not necessary to know the probability distribution of random data. This stems from the approach used in RO, where a solution is accepted if it is in a previous defined robustness space. Notice that under RO paradigm, it is not necessary to know the distribution of the data, instead, it is necessary to ensure that the solution is going to be inside the defined robustness space. The main advantages of this methodology lies on it is tailored to the information at hand, and allows computationally tractable formulations.

In this research a robust optimization approach was considered in order to deal with the randomness of the renewable sources. By doing so, power balance constrains were modeled as chance box constraints. With the purpose of understanding the aforementioned approach, several concepts are explained next.

4.1 Probability concepts

4.1.1 Deterministic and random variables

The set of variables that belong to a deterministic model are called deterministic variables. In this type of processes, the same inputs will produce invariably the same outputs. In other words, a deterministic variable can be known with complete exactitude. On the other hand, when an experiment is carried out, it is frequent that we are more interested in some function of the outcome as opposed to the actual outcome itself. These real-valued functions defined on the sample space, are known as random variables (Ross, 1998). Additionally, a random variable can be understood as a variable whose value cannot be known with complete exactitude.

4.1.2 Probability space

A probability space is a triple (H, $\mathfrak{B}$,$\mathfrak{P}$), where H is a nonempty space known as sample space, $\mathfrak{B}$ is a $\sigma-$algebra on H and $\mathfrak{P}$ is a function from H that represents the assignment of probabilities to the events (Schweizer and Sklar, 2005). All these definitions are explained in appendix C.

On the other hand, it is worth mentioning that the probability spaces that are used in this research correspond to those conformed by the sample space wind and solar power.

4.1.3 Probability density function

The probability density function (PDF) provides the probability to find the variable X in a infinitisimal interval dx. It is formally defined as:

$$f(x)dx = \text{Prob}\ (x \leq X \leq x + dx) \tag{4.1}$$

Where the area under $f(x)$ represents the total probability of having any observed value and must be equal to one (Gilchrist, 2000). An example of a PDF is shown in Figure 4.1. It is important to highlight that not all PDF are symmetric or unimodal as the one shown in this Figure.

4.1.4 Cumulative distribution function.

The cumulative distribution function, also called the distribution function F of a random variable X, for all real numbers $x, -\infty < x < \infty$ is defined as:

$$F(x) = Prob(X \leq x) \tag{4.2}$$

Summed up, $F(x)$ represents the probability that the random variable X takes on a value that is less than or equal to x, and its main characteristic is

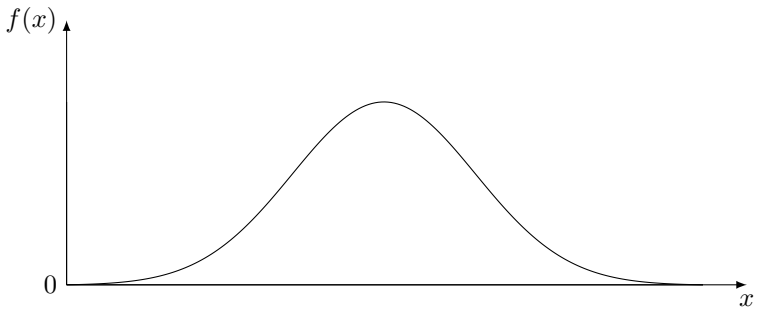

Figure 4.1: A probability density function

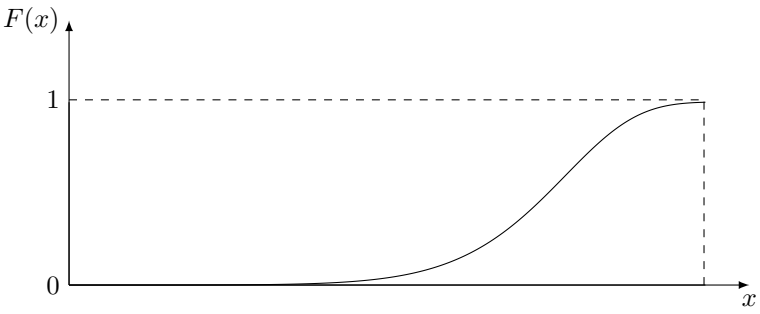

Figure 4.2: A cumulative distribution function

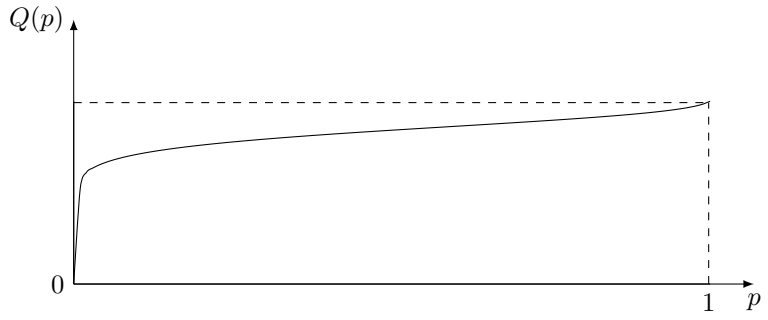

Figure 4.3: A quantile function

that it is always monotonically increasing (Ross, 1998). Notice that the relation between $f(x)$ and $F(x)$ is given by:

$$\int f(x)dx = F(x) \tag{4.3}$$

4.1.5 Quantile function

The quantile function is another way to represent a distribution (Gilchrist, 2000).Formally, it is defined as :

$$Q(p) = inf\{x \in \mathbb{R} : p \leq F(x_p)\} \tag{4.4}$$

Where x_p is the P-quantile of the population. The function $Q(p) = x_p$ is called the quantile function and represents the P-quantile as a function of p (Gilchrist, 2000). Notice that, the value x_p represents the value of x which $\text{Prob}\ (X \leq x_p) = p$. The relation between the quantile function and the cumulative distribution function is given as (Gilchrist, 2000):

$$Q(p) = F^{-1}(p) \tag{4.5}$$

$$F(x) = Q^{-1}(x) \tag{4.6}$$

4.2 Robust optimization

Let us consider a linear programming problem (LP) of the following form:

$$\text{minimize } c^\top X \tag{4.7}$$

$$\text{subject to } a^\top X \leq b \tag{4.8}$$

$$a^\top, b, c^\top \in \mathcal{M} \tag{4.9}$$

Where the data is comprised of the numerical values of the entries in ($c^\top$, $a^\top$, b) and varies in a given uncertain set $\mathcal{M}$. Robust optimization solves uncertain LP problems based on three assumptions on the underlying decision-marking environment:

A. All entries in the decision vector X represent "here and now" decisions: they should get specific numerical values as a result of solving the problem before the actual data “reveals itself.”

B. The decision maker is completely responsible for consequences of the decisions to be made when, and only when, the actual data is within the specified uncertainty set $\mathcal{M}$.

C. The constraints of the problem are hard. That is to say, violations of constraints, when the data is in $\mathcal{M}$, are not tolerated.

The aforementioned suppositions lead to the definition of an "immunized against uncertainty" solution on a uncertain problem. Notice that, assumption A imply that the vector X should be a fixed vector that, considering assumptions B and C, should remain feasible for the constraints regardless the realization of the data withing $\mathcal{M}$; such solutions is called "robust feasible". Consequently, in a decision-making environment, meaningfull solutions to a problem with uncertainties are its robust feasible solutions. It remains to interpret the value of the objective solutions. Thus, by considering the "worst-case-oriented" approach of robust optimization, it makes to quantify the quality of a robust feasible solution X by the "guaranteed" value of the original objective, this means, by its largest value $\sup\{c^\top x \leq b : (c, a^\top, b) \in \mathcal{M}\}$. In consequence, the best possible robust feasible solution is given by the solution of the following optimization problem:

$$\underset{X}{\text{minimize}}\{\sup_{(c,a^\top,b)\in\mathcal{M}} c^\top X\} \tag{4.10}$$

$$\text{subject to } a^\top X \leq b \; \forall \; (a^\top, b, c) \in \mathcal{M} \tag{4.11}$$

This optimization problem can be rewritten as:

$$\underset{X,z}{\text{minimize}} \quad z \tag{4.12}$$

$$\text{subject to } c^\top X \leq z \tag{4.13}$$

$$a^\top X \leq b \; \forall \; (a^\top, b, c) \in \mathcal{M} \tag{4.14}$$

The latter formulation is called the robust counterpart of the original uncertainty problem. This methodology, in its simplest version, proposes to associate with an uncertain problem its robust counterpart and using the associated robust optimal solutions as our “real life” decisions. Subsequently, Figure 4.4 depicts a sample space H with a robutness space $\mathcal{M}$. Notice that the optimization

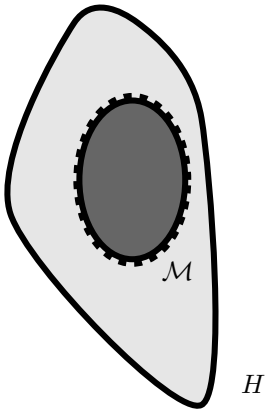

Figure 4.4: Sample space H and robustness space $\mathcal{M}$

problem is carried out inside the area surrounded by the dashed perimeter. For the studied problem H represents the set of values that the renewable power can take and $\mathcal{M}$ represents the subset of power values that we are willing to accept.

To summarize, robust optimization methodology optimizes over a "robustness space" (which is defined by the decision maker) of the original sample space, under the “worst-case-oriented” philosophy (Aharon Ben-Tal and Nemirovski, 2009). In adittion, the aforementioned formulation can be carried out by only considering the stochasticity of b, in this case the parameters $a^\top$ and c are known while $b \in \mathcal{M}$. This will be the approach that we will we use to model the equations with random variables of our problem.

It is important to highlight that the previous formulation can be extended to QCQP problems by considering the explanation given in Chapter 3.

4.3 Chance box constraint

let us consider the following structure for an optimization problem:

$$\text{minimize } f_0(Y) \tag{4.15}$$
$$\text{subject to } a_t \leq Y_t \leq l_t \;\; t = 1, ..., T \tag{4.16}$$

where Y is the variable. The constrains can be called *variable bounds* (since they give lower and upper bounds for each Y_i) or *box constraints* (since the feasible set is a box). This problem can be also expressed as (Boyd and Vndenberghe, 2009):

$$\text{minimize } f_0(Y) \tag{4.17}$$
$$\text{subject to } a_t \leq Y_t \tag{4.18}$$
$$l_t \geq Y_t \quad t = 1, ..., T \tag{4.19}$$

When Y_t is an aleatory variable, the aforementioned constraints are called chance box constraints. The way to deal with these kind of restrictions is explained next.

4.3.1 Chance box constraint definition

A constraint of the form:

$$X_t \geq D_t, \quad t = 1, ..., T. \tag{4.20}$$

Requires a probabilistic approach when X_t is random and D_t is deterministic. Thus, Constraint (4.20) is expressed as a chance constraint of the form of Equation (4.21), which states that the probability of X_t equaling or exceeding D_t is at least equal to a given parameter ζ, this means that at least ζ percent of the time X_t must be greater than or equal to D_t.

$$\text{Prob}\ (X_t \geq D_t) \geq \zeta_t, \quad t = 1, ..., T. \tag{4.21}$$

Notice that (4.21) can be rewritten as (4.22) if we consider that $\text{Prob}[D_t \leq a] + \text{Prob}[D_t \geq a] = 1$.

$$\text{Prob}\ (X_t \leq D_t) \leq 1 - \zeta_t, \quad t = 1, ..., T. \tag{4.22}$$

Considering the definition given in section 4.1.4, Equation (4.22) can be written:

$$F_{X_t}(D_t) \leq 1 - \zeta_t \tag{4.23}$$

Where $F_{X_t}(D_t)$ is the cumulative distribution function of X_t evaluated in D_t.

The aforementioned formulation allows us to obtain a deterministic equivalent for the probabilistic constraint represented by Equation (4.21)(S Vedula, 2007). Said deterministic equivalent is given as:

$$F_{X_t}^{-1}(1 - \zeta_t) \geq D_t \tag{4.24}$$

Where $F_{X_t}^{-1}$ is the quantile function explained in section 4.1.5. It is important to emphasize that constraints of the form (4.24) fit with the convexity criteria.

4.3.2 Considering stochasticity of renewable sources into the STHS

Equations (3.80), (3.81), (3.84) and (3.85) used in the deterministic model IV do not consider the random nature of renewable sources. Therefore, a model which considers the stochastic behavior of the sources is needed. In this way, constraint (3.65) can be written as:

$$\text{Prob}\ (P^{k,t}_{G_{P.U}} \geq F^{k,t}_{Ft_{P.U}}) \geq \zeta_t \ for\ k = u, e \tag{4.25}$$

Similarly, the stochasticity of the demand can be considered by considering nodes with loads, such as the ones represented by Equation (3.64), as follows:

$$\text{Prob}\ (F^{k,t}_{St_{P.U}} - \sum_{n \in N_k} F^{k,n,t}_{L_{P.U}} \geq P^{k,t}_{D_{P.U}}) \geq \zeta_t \tag{4.26}$$

It is important to emphasize that the equality constraints with random variables were changed for inequality constraints that should hold with a probability exceeding ζ_t(Equations (4.25) and (4.26)). In doing so, these equation can be modeled as chance box constraints.

4.3.3 Flow balance as a chance box constraint

Let us consider Equation (4.25). First, where $P^{k,t}_{G}$ is the random variable. In this case equations (4.21), (4.22), (4.23) and (4.24) take the form of:

$$\text{Prob}\ (P^{k,t}_{G_{P.U}} \geq F^{k,t}_{Ft_{P.U}}) \geq \zeta_t \tag{4.27}$$

$$\text{Prob}\ (P^{k,t}_{G_{P.U}} \leq F^{k,t}_{Ft_{P.U}}) \leq 1 - \zeta_t \tag{4.28}$$

$$F_{P^{k,t}_{G_{P.U}}}\ (F^{k,t}_{Ft_{P.U}}) \leq 1 - \zeta_t \tag{4.29}$$

$$F^{-1}_{P^{k,t}_{G_{P.U}}}\ (1 - \zeta_t) \geq F^{k,t}_{Ft_{P.U}} \tag{4.30}$$

Similarly, an expression for Equation (4.26) can be deduced, where the random variable is $P^{k,t}_{D}$. Notice that this equation is equivalent to:

$$\text{Prob}\ (P^{k,t}_{D_{P.U}} \leq F^{k,t}_{St_{P.U}} - \sum_{n \in N_k} F^{k,n,t}_{L_{P.U}}) \geq \zeta_t \tag{4.31}$$

It is important to say that the left term of Equation (4.31) already has the form of Equation (4.2), so changing the inequality in the left term of the equation is not necessary. Thus, this equation can be rewritten as:

$$F_{P^{k,t}_{D_{P.U}}}(F^{k,t}_{St_{P.U}} - \sum_{n\in N_k} F^{k,n,t}_{L_{P.U}}) \geq \zeta_t \tag{4.32}$$

$$F^{k,t}_{St_{P.U}} - \sum_{n\in N_k} F^{k,n,t}_{L_{P.U}} \geq F^{-1}_{P^{k,t}_{D_{P.U}}}(\zeta_t) \tag{4.33}$$

$$F^{k,t}_{St_{P.U}} \geq F^{-1}_{P^{k,t}_{D_{P.U}}}(\zeta_t) + \sum_{n\in N_k} F^{k,n,t}_{L_{P.U}} \tag{4.34}$$

On one hand Equation (4.30) allows us to consider the stochasticity of renewable resources when the node k is a node connected to a wind or a solar unit. On the other hand, (4.34) considers the stochastic behavior of load. Both, (4.30) and (4.34) are deterministic equivalents for the original equations.

4.4 Stochasticity of the radom variables

4.4.1 Stochastic behavior of wind and wind power data

One of the main challenges of wind generation is the stochasticity of wind since said stochasticity makes impossible predicting the amount of power that can be generated with this units with exactitude. This produces that the equilibrium between power production and power consumed cannot be guaranteed. In order to try modeling the behavior of this aleatory variable, wind speed data are fitted to a Weibull distribution (see Figure 4.5) which is defined as follows:

$$f(v_w) = \frac{\kappa_w}{c_w}\left(\frac{v_w}{c_w}\right)^{\kappa_w - 1} e^{-\left(\frac{v_w}{c_w}\right)^{\kappa_w}} \tag{4.35}$$

Where c_w and κ_w are the scale and shape factor. It is important to emphasize that the aforementioned equation corresponds with the probability density function of wind, however the variable that concern us in the STHS problem is wind power (Equation (2.11)) which is also a stochastic variable. An example of a wind probability density function is shown in Figure 4.6. Notice that the great peak that corresponds to $P_w = 0$ makes sense if we consider that wind turbines do not produce power in the interval $[V_w = 0, V_w = V_{Cut-in}]$. Next, there is a great concentration of data around the power that corresponds to the rated value of wind data. Finally, there is a small peak in $P_w = P_{w-rated}$, the reason for this is that the wind speed data used to create this curve reach V_{rated} occasionally. This graphic can change depending on the wind speed behavior.

The aforementioned said implies that the probability density, cummulative density and quantile functions are going to be influenced by the piecewise linear properties of Equation (2.11). For sake of simplicity, these functions are

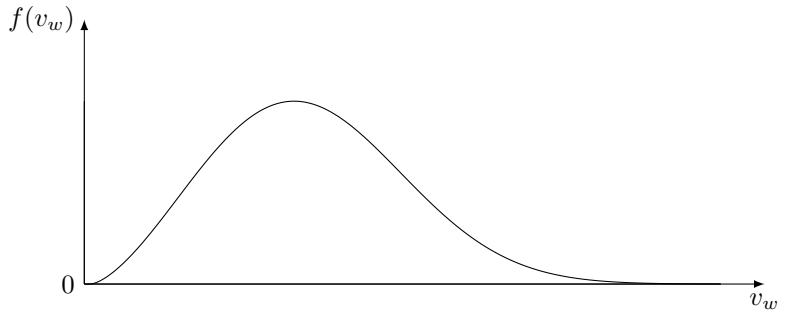

Figure 4.5: Probability density function of wind speed

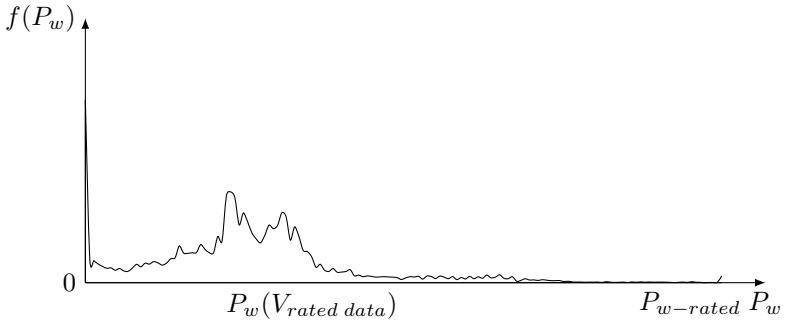

Figure 4.6: Probability density function of wind power

calculated in a numeric way.

It is important to emphasize that the latter behavior corresponds for data per hour.

4.4.2 Stochasctic behavior of solar power data

Capacity factor of a solar power plant is strongly influenced by the solar radiation levels of the place where these were measured. The probability distribution function of this capacity factors fits with a Weibull distribution as Figure 4.7 depicts. The probability density function of the output power will be the same as the probability density function of the capacity factor times $P_{S_{rated}}$.

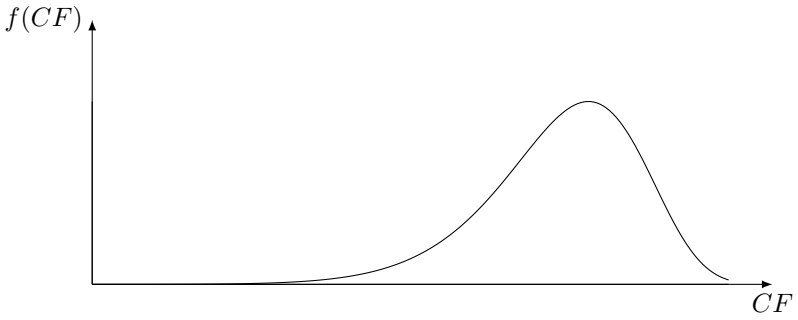

Figure 4.7: Probability density function of solar capacity factor

4.4.3 Stochasctic behavior of load

The power consumed of an electrical power system is a variable that cannot be forecast with exactitud. The reason for this is that the load depends on the will of the consumer to turn on and turn off their electrical devices. However, the behavior of the demand is strongly attached to some humans behavior patterns, which allows load demand forecasts be accurate with a deviation around 5%. This makes possible modeling the electrical energy consume for a period t as an uniform distribution, which is formulated as follows:

$$f(x) = \begin{cases} \frac{x-o}{s-o} & o \leq x \leq s \\ \\ 0 & otherwise \end{cases} \tag{4.36}$$

.

From definitions 4.1.4 and 4.1.5 it is easy to see that the quantile function for the uniform distribution can be written as:

$$Q(p) = (1-p)o + ps \tag{4.37}$$

Notice that the values o and s correspond to the values between the load forecast varies. This means $o = \overline{P_D} + 0.05\overline{P_D}$ and $s = \overline{P_D} - 0.05\overline{P_D}$, Figure 4.8 depicts this behavior.

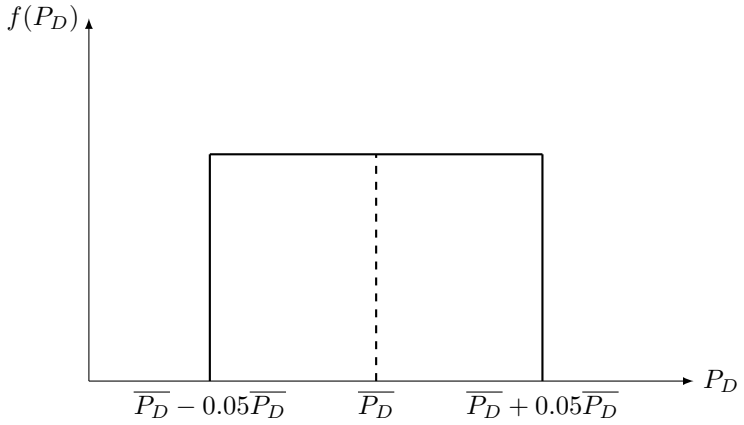

Figure 4.8: Uniform probability distribution function

4.5 Robust hydrothermal-wind-solar coordination model (Model V)

The short-term hydrothermal-wind-solar coordination model that consider the stochasticity of wind and solar generation is presented as follows:

$$\text{Minimize } z \tag{4.38}$$

Subject to:

$$\sum_{t\in\Omega}\sum_{i\in\Delta}\left\|(\gamma^i)^{1/2}P_{base}P^{i,t}_{Th_{P.U}} + (\gamma^i)^{1/2}\frac{\beta^i}{2}\right\| \leq z \tag{4.39}$$

- Active Power balance

$$P^{k,t}_{G_{P.U}} = F^{k,t}_{Ft_{P.U}} \quad k = i,j \tag{4.40}$$

$$F^{k,t}_{Ft_{P.U}} = F^{k,t}_{St_{P.U}} \tag{4.41}$$

$$F^{-1}_{P^{k,t}_{G_{P.U}}}(1-\zeta_t) \geq F^{k,t}_{Ft_{P.U}} \quad k = e,u \tag{4.42}$$

$$F_{St_{P.U}}^{k,t} \geq F_{P_{D_{P.U}}^{k,t}}^{-1}(\zeta_t) + \sum_{n \in N_k} F_{L_{P.U}}^{k,n,t} \tag{4.43}$$

$$F_{St_{P.U}}^{k,t} = \sum_{n \in N_k} F_{L_{P.U}}^{k,n,t} \tag{4.44}$$

- Power flow constraints

$$[P_{G_{P.U}}]^t - [F_{P_{D_{P.U}}}^{-1}(\zeta)]^t = [B_{P.U}][\theta]^t \tag{4.45}$$

$$F_{L_{P.U}}^{k,n,t} = \frac{\theta^{k,t} - \theta^{n,t}}{X_{k,n}} \tag{4.46}$$

$$F_{L_{Tmin\ P.U}}^{k,n} \leq F_{L_{P.U}}^{k,n,t} \leq F_{L_{Tmax\ P.U}}^{k,n} \tag{4.47}$$

$$-\frac{\pi}{2} \leq \theta^{k,n,t} \leq \frac{\pi}{2} \tag{4.48}$$

- Generated power

$$P_{G_{P.U}}^{i,t} = P_{Th_{P.U}}^{i,t} \tag{4.49}$$

$$P_{G_{P.U}}^{j,t} = P_{H_{P.U}}^{j,t} \tag{4.50}$$

$$P_{G_{P.U}}^{e,t} = F_{P_{w_{P.U}}^{e,t}}^{-1}(1 - \zeta_t) \tag{4.51}$$

$$P_{G_{P.U}}^{u,t} = F_{P_{S_{P.U}}^{u,t}}^{-1}(1 - \zeta_t) \tag{4.52}$$

- Hydroelectric generation (SOC)

$$\left\| \begin{pmatrix} \frac{1 - \begin{pmatrix} C_{4_{P.U}}^j \\ C_{5_{p.u}}^j \end{pmatrix}^\top \begin{pmatrix} Q_{P.U}^{j,t} \\ V_{P.U}^{j,t} \end{pmatrix} - C_{6_{p.u}}^j + P_{H_{P.U}}^{j,t}}{2} \\ \begin{pmatrix} -C_{1_{P.U}}^j & \frac{-C_{3_{P.U}}{}^j}{2} \\ \frac{-C_{3_{P.U}}{}^j}{2} & -C_{2_{P.U}}^j \end{pmatrix}^{\frac{1}{2}} \begin{pmatrix} Q_{P.U}^{j,t} \\ V_{P.U}^{j,t} \end{pmatrix} \end{pmatrix} \right\| \leq \mathfrak{U}_{P.U} \tag{4.53}$$

Where the value of $\mathfrak{U}$ is given by Equation 3.21.

- Continuity equation for the hydro reservoir network

$$V_{P.U}^{j,t} = V_{P.U}^{j,t-1} + I_{P.U}^{j,t} - Q_{P.U}^{j,t} - S_{P.U}^{j,t} + \sum_{\pi \in S_{\Omega j}} (Q_{P.U}^{\pi,t-\tau} + S_{P.U}^{\pi,t-\tau}) \tag{4.54}$$

$$V_{P.U}^{j,0} = V_{ini_{P.U}}^{j} \tag{4.55}$$

$$V_{P.U}^{j,T} = V_{end_{P.U}}^{j} \tag{4.56}$$

- Physical limitations on reservoir storage volumes, discharge rates and power generation

$$V_{min_{P.U}}^{j} \leq V_{P.U}^{j,t} \leq V_{max_{P.U}}^{j} \tag{4.57}$$

$$Q_{min_{P.U}}^{j} \leq Q_{P.U}^{j,t} \leq Q_{max_{P.U}}^{j} \tag{4.58}$$

$$P_{Th_{min_{P.U}}}^{i} \leq P_{Th_{P.U}}^{i,t} \leq P_{Th_{max_{P.U}}}^{i} \tag{4.59}$$

$$P_{H_{min_{P.U}}}^{j} \leq P_{H_{P.U}}^{j,t} \leq P_{H_{max_{P.U}}}^{j} \tag{4.60}$$

$$S_{min_{P.U}}^{j} \leq S_{P.U}^{j,t} \leq S_{max_{P.U}}^{j} \tag{4.61}$$

Notice that the values of load demand and power produced by renewable sources were replaced by their quantile functions evaluated in ζ and $(\zeta - 1)$ respectively. In addition, Equations (4.43) corresponds to the nodes where there is load, while Equation (4.44) corresponds to the secondary of transformers where load does not exist.

It is important highlight that quantile functions of wind power and solar power were built with data from data bases. Furthermore, quantile function of demanded power was built as it is explained in subsection 4.4.3. Otherwise, the chance box constraints (4.42) and (4.43) are convex too.

Chapter 5

Results

Three sets of simulations were carried out in order to test the proposed models and compare them. First, it was only consider a hydrothermal system (Model II) in order to compare the obtained results with previous research that had used the same test system. In this model, the spillage was considered equal to zero as previous research did before. It is important to highlight that the proposed convex model is an approximation of the real model. Therefore, the comparison must be performed in terms of both time calculation and accuracy of the solution.

Then, a convex-deterministic short-term hydrothermal-wind solar model was tested without considering the stochastic nature of the renewable resources and load (Model IV, case I). Additionally, constrains related to the grid were considered with the DC power flow approximation (Model IV, case II).

Next, a stochastic model was implemented by considering a robust set of 80% to hold the chance constraint of this model (Model V, case I). Finally, the same model was tested but, in this case, the probability to hold the chance constraints was considered 60% (Model V, case II).

It is important to highlight that for Models IV and V the upper limits of spillage was considered equal to $2 \times 10^4 \frac{m^3}{h}$ in order to have a more realistic model and study how these variables affect the optimization problem. All data of the test systems used are presented in Appendix A. All cases were implemented in command line of Matlab R2017b by using CVX and Sedumi solver in a 3.2 GHz, Intel Core i8-8700, with 8 GB RAM PC.

For sake of completeness the models used are summarized in Table 5.1.

Model	Description
Model I	STHS-non-convex
Model II	STHS-SOC aproximation, S=0
Model III	STHS-convex with grid
Model IV Case I	STHS-deterministic, convex, with grid, renewable energy y without grid constraint
Model IV, Case II	STHS-deterministic,convex,with grid, renewable energy and without grid constraint
Model V Case I	STHS-robusto,convex,with grid, renewable energy and without grid constraint
Model V Case II	STHS-robusto,convex,with grid, renewable energy and without grid constraint

Table 5.1: Models resume

5.1 Results Model II

In order to have a framework to compare time convergence and accuracy of the proposed methodology, the short-term scheduling was carried out without considering renewable resources nor the grid. In doing so, Model II was tested. For sake of simplicity, only time convergence and the value of the objective function are compared. Table 5.2 shows a comparison of results obtained for several methodologies implemented in the test system presented in (Orero and Irving, 1998).

It is not difficult to see that SOC presents a superior performance regarding time convergence compared with other methauristic techniques and linearizations proposed in the past. In addition, SOC and semidefinite programming find the same optimum which is one of the main characteristics of convex optimization.

It is worth mentioning that the results of metaheuristic techniques presented in Table 5.2 give us just an idea about the possible solution of the problem; these techniques do not guarantee global optimum since their operation depends more on luck than on a mathematical model. The exact solution of non-convex optimization problems is still an open problem. therefore, there is no way to carry out an exact comparison regarding to the value of the objective function.

5.2 Results Model IV

For the model that considers the grid, wind and solar generation, with the nominal values of power capacity of the lines (Model IV Case I), the values of wind speed and solar capacity were considered as the mean value of the data per hour.

From Figures 5.1, 5.2 and 5.5 it can be observed that the amount of energy produced by unit 3 tends to be low in some intervals, even though the volume and the water discharge are not low, which seems to contradict Equation (2.20), where the hydro power is proportional to the water discharges and the volume of the reservoirs. Nevertheless, this behavior makes sense if we consider that the coefficients C_i^j of unit 3 are the smallest value compared with the others,

Methodology	Objective function value (CU)	CPU time (s)
SOC Model II	925866.00	4.7
SDP I (Yunan Zhu and Yang, 2013)	925866.00	———-
APSO(Amjady and Soleymanpour, 2010)	926151.54	———-
LCPSO (B. Yu and Wang, 2007)	926651.4	103.5
LWPSO (B. Yu and Wang, 2007)	926352.8	82.9
IPSO (P.K. Hota and Chakrabarti, 2009)	922553.49	———-
CPSO (Yuqiang Wua and Liu, 2019)	922328.64	18.6
PSO (Xiaohui Yuan, 2008)	928878.00	———-
EPSO (Xiaohui Yuan, 2008)	922904.00	———-
SPPSO (J. Zhang and Yue, 2012)	922336.31	16.3
DE (Manda and Chakraborty, 2008)	923991.08	14.50
DE (Yongqiang Wang and Zhang, 2012)	923234.56	8.69
DRQEA (Yongqiang Wang and Zhang, 2012)	922526.73	7.98
ACDE (Youlin Lu and Zhang, 2010)	924661.53	7
GA (Orero and Irving, 1998)	938370.00	3720
BCGA (Kumar and Naresh, 2007)	927815.35	64.51
RCGA (Kumar and Naresh, 2007)	926120.26	57.52
CDE (Youlin Lu and Zhang, 2010)	926833.98	7
CEP (Nidul Sinha and Chattopadhyay, 2003)	930373.23	2292.1
MHDE (Lakshminarasimman and Subramanian, 2008)	921 893.94	8
FEP (Nidul Sinha and Chattopadhyay, 2003)	930897.44	1911.2
IFEP (Nidul Sinha and Chattopadhyay, 2003)	930290.13	1033.2
EGA (Xiaohui Yuan, 2008)	934727.00	———-
SOS (Sujoy Das and Chakraborty, 2018b)	922338.20	6.21
QRSOS (Sujoy Das and Chakraborty, 2018b)	922329.94	5.16

Table 5.2: Optimal cost and CPU time of SOC and other methodologies

this means that unit 3 is the unit with less rated power of the hydrochain.

In addition, Figures 5.1, 5.2, 5.3 and 5.5 show that the optimization model tends to reduce the volume of reservoir 3 (without violating the final values of the volume) while the volume of reservoir 4 increases. The reason for this is that unit 4 is more capable to produce power than unit 3 (Interested reader can evaluate Equation (2.20) with the coefficients of unit 3 and unit 4 and will notice that, for the same values of volume and water discharges, the produced power by unit 4 will be larger than the produced power of unit 3). That is why the model tends to produce power by using unit 4 rather than unit 3. Thus, the spillage of the reservoir 3 tends to be as large as possible until the volume of the reservoir 4 needs to decrease to reach the final value. Besides, analyzing the dual variables of the upper bound of spillage can be useful to understand this behavior better. Figure 5.9 depicts the rate of change of the objective function with respect to the upper bound of spillage. Notice that this dual variable for reservoir 3 impacts considerably the objective function, while dual variables of reservoir 1, 2 and 4 do not do it. This implies that allowing spillage be different to zero can decrease the operation cost of the power system.It is important to highlight that this kind of analysis cannot be carried out when heuristic and metaheuristic techniques are used.

On the other hand, Figure 5.6 shows wind power behavior which reaches

its peaks of power production in the intervals of time between 10-12 hours and between 22-24 hours. This behavior is due the particular characteristics of the wind resource in the place where the data were measured. Under other conditions, Figure 5.7 shows that the peak of solar generation is between 10 and 13 hours, this shaves the peak of thermal power produced between this interval of time. Moreover, the solar production continue until 18 hours, this makes that the production of thermal power has to increase quickly in order to supply the maximum power consumption at 20 hours (see Figures 5.4 and 5.8).

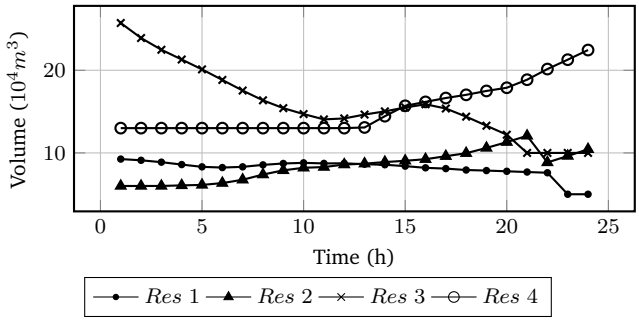

Figure 5.1: water discharge of hydro units (Model IV, case I)

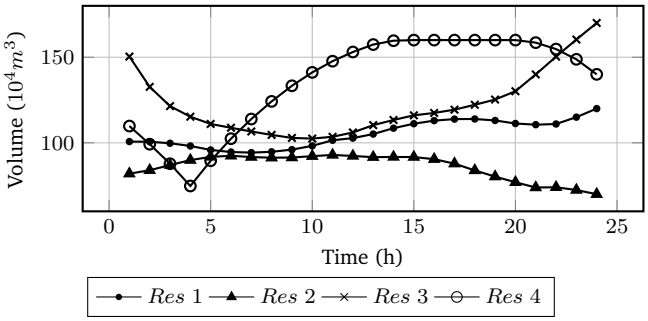

Figure 5.2: volumes of reservoirs (Model IV, case I)

In order to analyze how the grid can affect the generation scheduling, the capability of the line that connects generator 4 with the grid (line between nodes 39 and 36) was reduced. From Figures 5.6, 5.7, 5.15 and 5.16 it can be seen that modifying the line 39-36 does not affect the production of wind and solar power since the system is highly meshed and the power that comes from these generators can flow without any problems. The situation is similar for hydro units 1,2 and 3. However, it changes for hydro unit 4, in this case the unit produces power to supply the load located at node 39 which represents 10% of the total load of the system. Once the unit generates enough power to supply

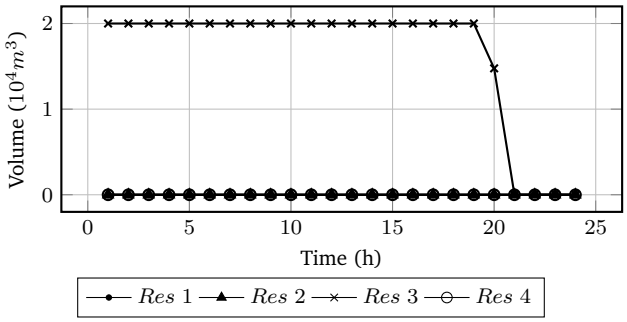

Figure 5.3: spillage (Model IV, case I)

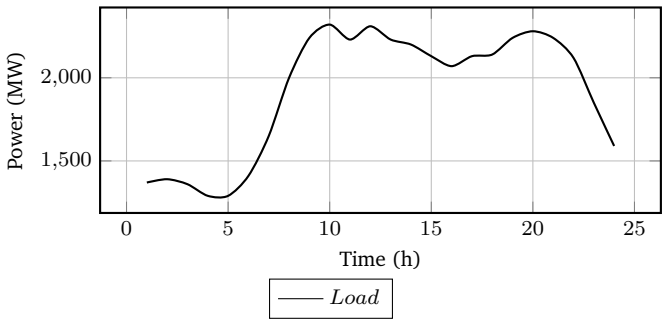

Figure 5.4: Power consumed (Model IV, case I)

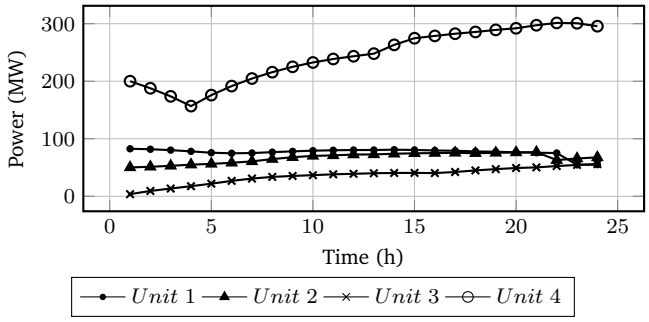

Figure 5.5: Power produced by hydro units (Model IV, case I)

the load, the surplus power is delivered to the interconnected system as long as line 39-36 is able to transport said power. However, if the amount of generated power is larger than the load requirements and the capability of the line, the generation of power has to be modified, compared with the produced power in Model IV case I, in order not to exceed the limit of power of the line. This behavior modifies the production of power of hydro unit 4 and thermal unit (see

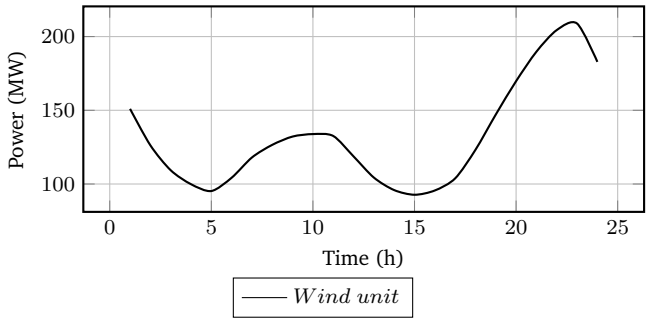

Figure 5.6: Power produced by wind unit (Model IV, case I)

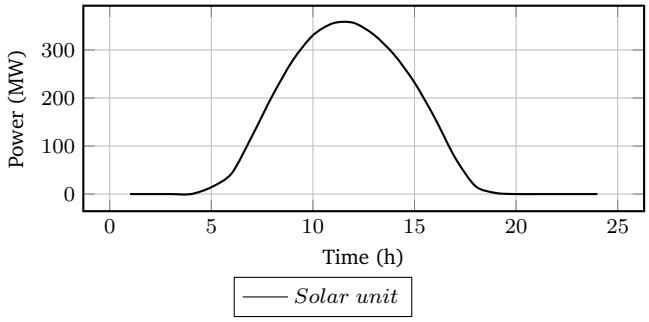

Figure 5.7: Power produced by solar unit (Model IV, case I)

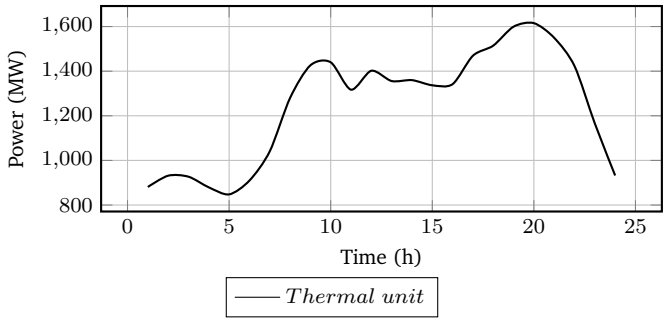

Figure 5.8: Power produced by thermal unit (Model IV, case I)

Figures 5.14 and 5.17), since the power that is not generated by hydroelectric 4 has to be supplied by thermal unit in order to supply the requirements of the load, which increases the operation cost of the system compared to Model IV case I (see Table 5.4). Moreover, this modifies the water discharges, the operation of reservoirs, the spillage and the impact of said spillage on the objective function as Figures 5.10, 5.11, 5.12 and 5.18 depict.

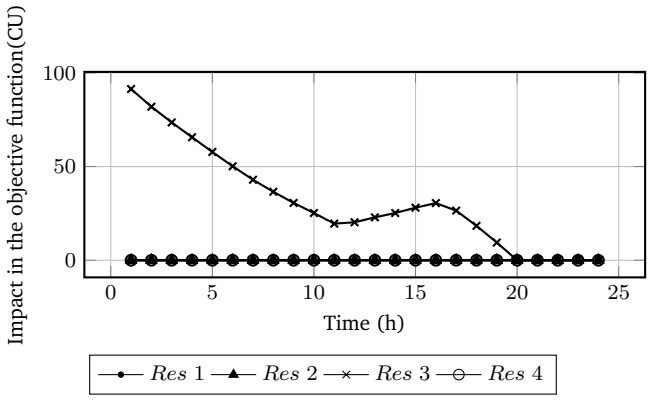

Figure 5.9: Dual variable of spillage (Model IV, case I)

By comparing the behavior of dual variables in both case of the Model IV (See figures 5.9 and 5.18), it is not difficult to see that the impact of the upper limit of the spillage of reservoir 3, on the objective function, decreases considerably in case II. The reason for this is that spilling water on the reservoir 4 is not that convenient as it used to be since the the low capacity of the line 39-36 which, in case II, constraints the capability of unit 4 to produce power.

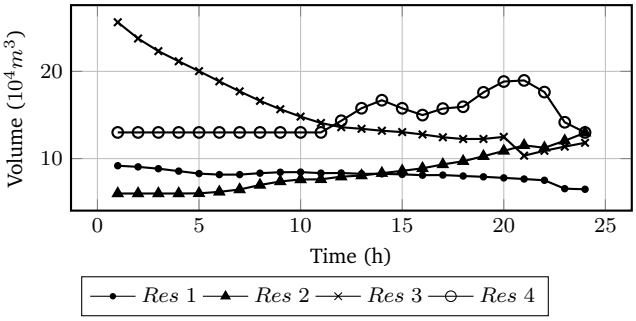

Figure 5.10: water discharge of hydro units (Model IV, case II)

5.3 Results Model V

This model was used to evaluate two cases: First the ζ values were set in 80% (Model V, case I). Then, they were set in 60% (Model V, case II) in order to see how the results change when these parameters change. It is important to higlight that the values of the quantile function can be calculated by using Equation (4.4). However, for sake of simplicity the function *quantile* of matlab was

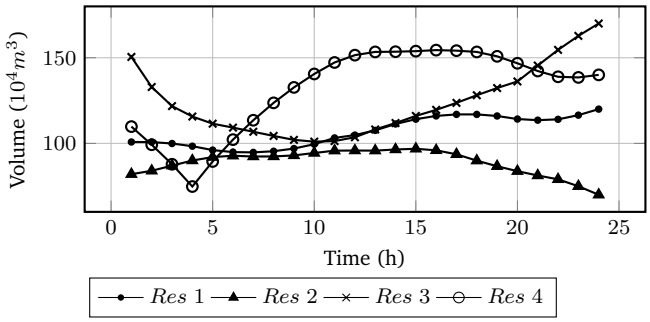

Figure 5.11: volumes of reservoirs (Model IV, case II)

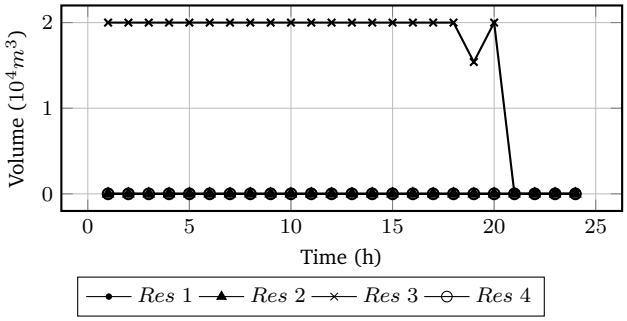

Figure 5.12: spillage (Model IV, case II)

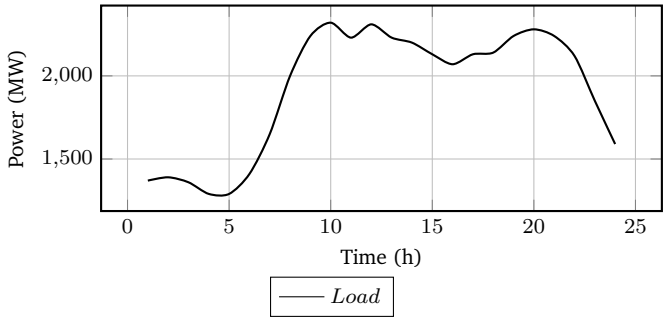

Figure 5.13: Power consumed (Model IV, case II)

used.

In both cases the behavior of hydro generation are the same compared to Model IV, case I. The reason why it does not change is that considering the stochasticity of the load, wind and solar generation, in the optimization model, is going to affect the thermal power production, which is the only variable that

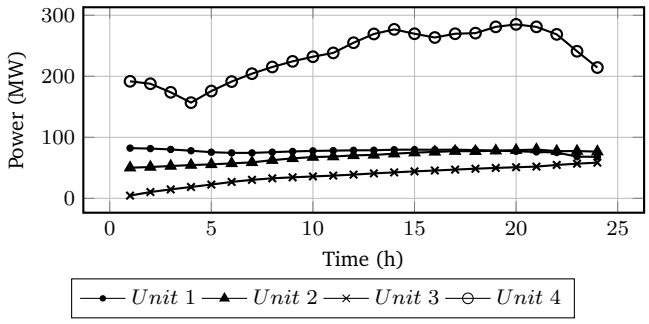

Figure 5.14: Power produced by hydro units (Model IV, case II)

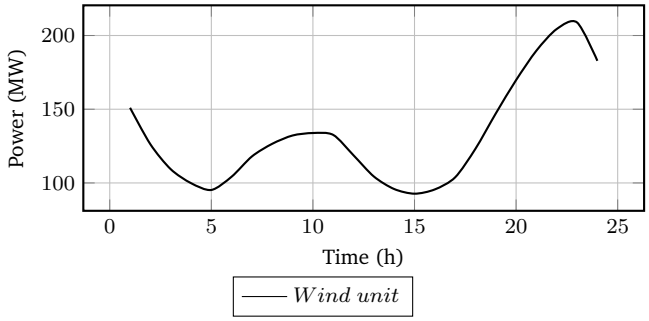

Figure 5.15: Power produced by wind unit (Model IV, case II)

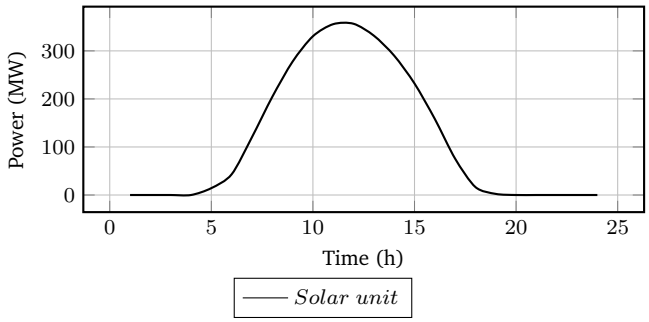

Figure 5.16: Power produced by solar unit (Model IV, case II)

affects directly the value of the objective function since the water cost are considered zero. Thus, water discharges (Figures 5.19 and 5.28) volume of reservoirs (Figures 5.20 and 5.29), spillage (Figures 5.21 and 5.30) and dual variable of upper limit of spillage (Figures 5.27 and 5.36) remain the same.

On the other hand, load demand (Figures 5.22 and 5.31), wind genera-

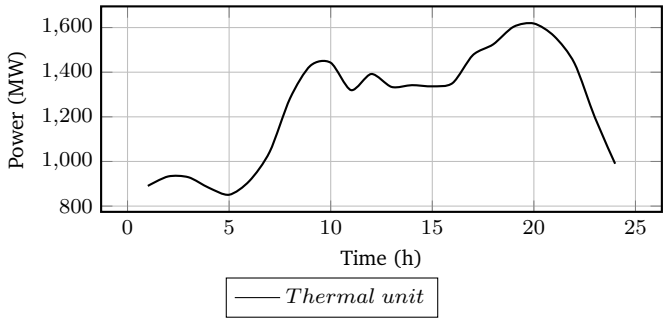

Figure 5.17: Power produced by thermal unit (Model IV, case II)

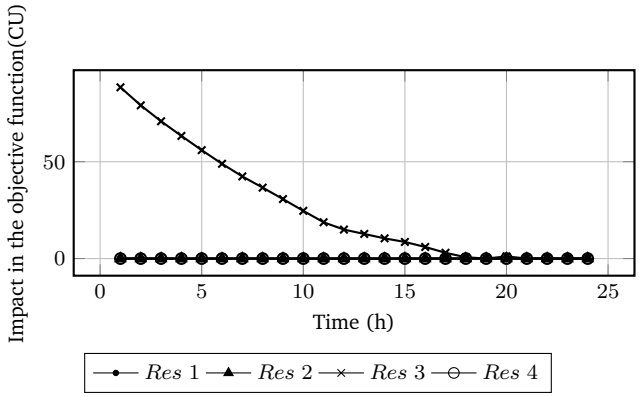

Figure 5.18: Dual variable of spillage (Model IV, case II)

tion (Figures 5.24 and 5.33) and solar generation (Figures 5.25 and 5.34) are modified when the stochasticity of these random variable is considered. This modify the generation of thermal power (Figures 5.26 and 5.35) which changes the value of the objective function, that is directly linked with the value of this variable. An analysis with more details is carried out in the next section.

5.4 Other results

It is important to mention that several simulations (for each model) were carried out in order to verify the uniqueness of the proposed methodology, all simulations gave the same optimal value, these values are presented in Table 5.4.

Figures 5.37 and 5.38 present a comparison between Model II and Model IV case I, where the production of thermal and hydro power are compared for both cases. Notice that the production of hydro power is the same in both cases, while the production of thermal power does change. This behavior is a result

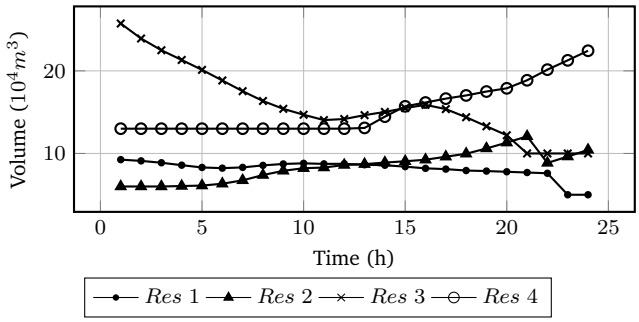

Figure 5.19: water discharge of hydro units (Model V, case I)

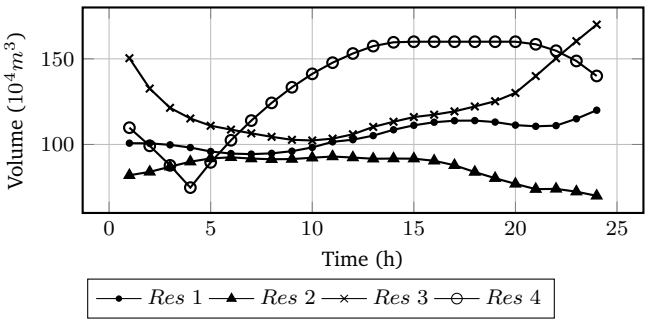

Figure 5.20: volumes of reservoirs (Model V, case I)

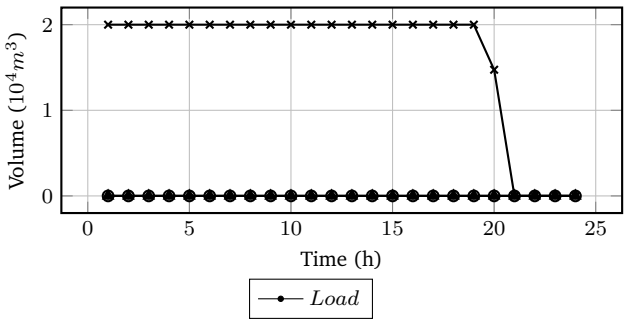

Figure 5.21: spillage (Model V, case I)

of the optimization process, which tends to reduce the power produced by thermal units instead of the production of hydro units, when renewable sources are considered. The reason for this is that the thermal production has an associated cost while the associated costs for hydro power plants are zero. Thus, the larger the renewable power is, the lower the thermal power is, until the lower limit of thermal unit and line capacities allow it.

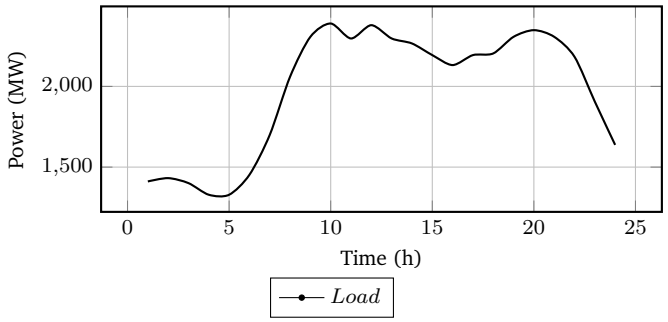

Figure 5.22: Power consumed (Model V, case I)

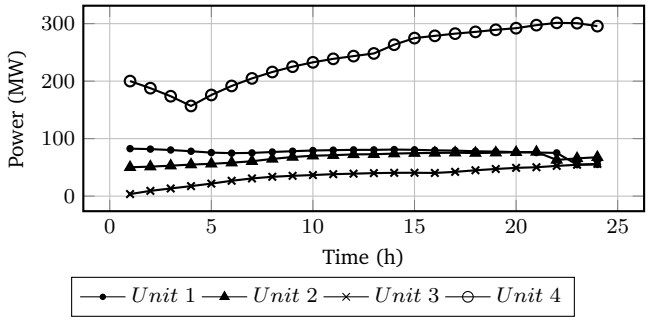

Figure 5.23: Power produced by hydro units (Model V, case I)

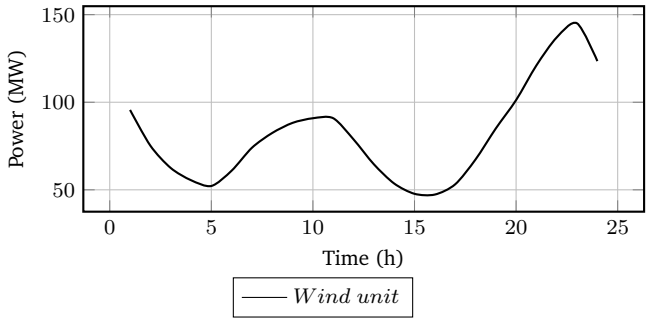

Figure 5.24: Power produced by wind unit (Model V, case I)

On the other hand, Figures 5.43, 5.44 and 5.45 depicts the quantile function for wind power, solar power and power consumed. For sake of simplicity these figures were drawn just for an hour since the quantile functions keep the same shape for all hours, except for the function of solar power at hours when there is no solar radiation. In this case, said function is a straight line located in

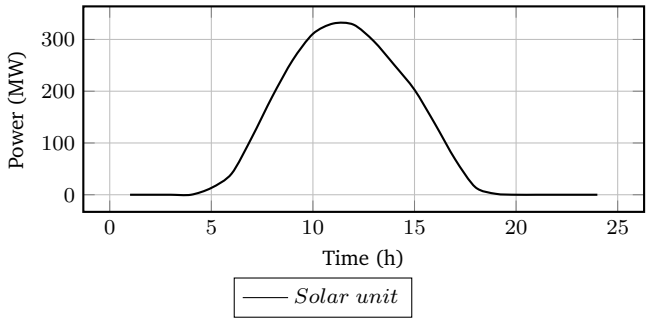

Figure 5.25: Power produced by solar unit (Model V, case I)

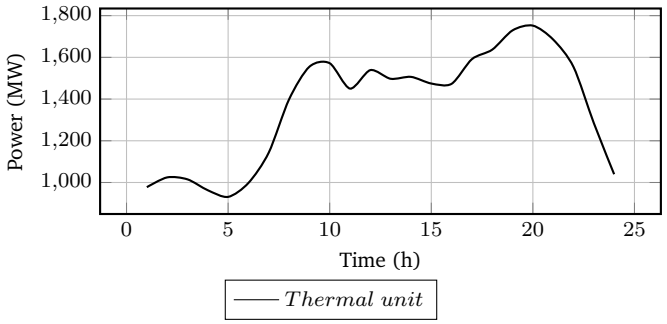

Figure 5.26: Power produced by thermal unit (Model V, case I)

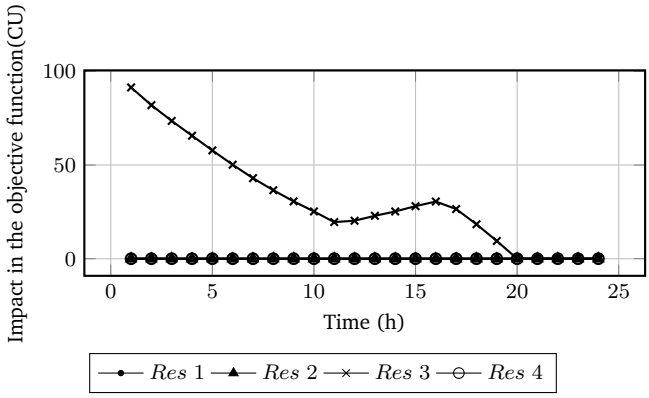

Figure 5.27: Dual variable of spillage (Model V, case I)

$Q(p) = 0$. It is easy to see that the reason for this is that the power produced in this period is equal to zero.

Both, the quantile functions of solar and wind power (see Figures 5.43 and

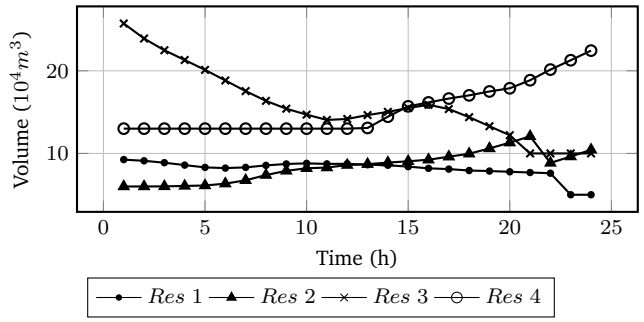

Figure 5.28: water discharge of hydro units (Model V, case II)

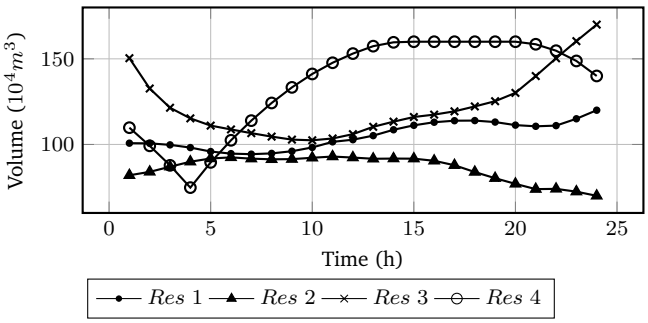

Figure 5.29: volumes of reservoirs (Model V, case II)

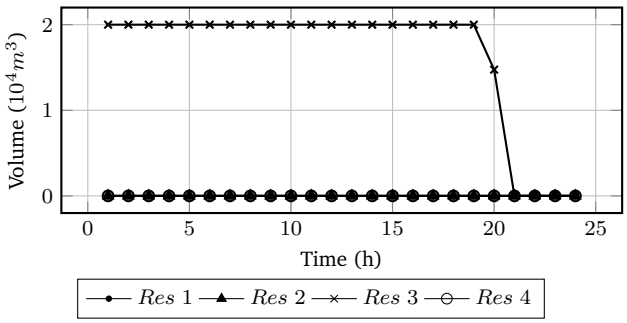

Figure 5.30: spillage (Model V, case II)

5.44) show that, if it is required to hold constraints (4.51) and (4.52) with a higher probability, the value of $Q(p)$ is going to be lower. The reasons for this is that, as ζ increases, the value $1-\zeta$ decreases which produces a movement to the left in both figures. This implies that, in the quantile function which is always growing, the value of $Q(p)$ decreases when a movement to the left is carried out. Consequently, when $\zeta = 80\%$ both, wind and solar generation, are

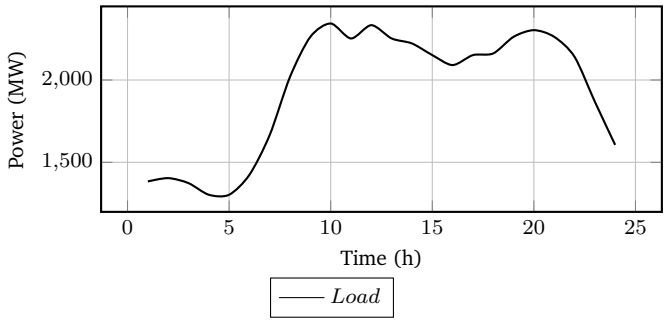

Figure 5.31: Power consumed (Model V, case II)

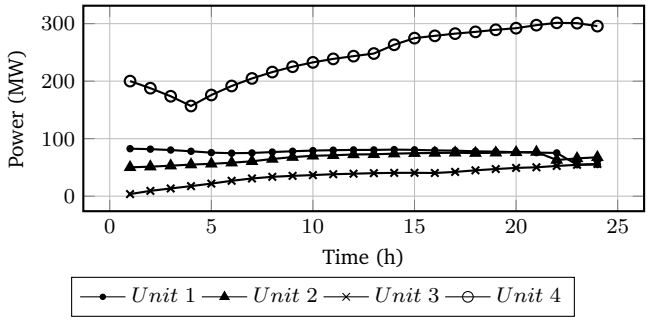

Figure 5.32: Power produced by hydro units (Model V, case II)

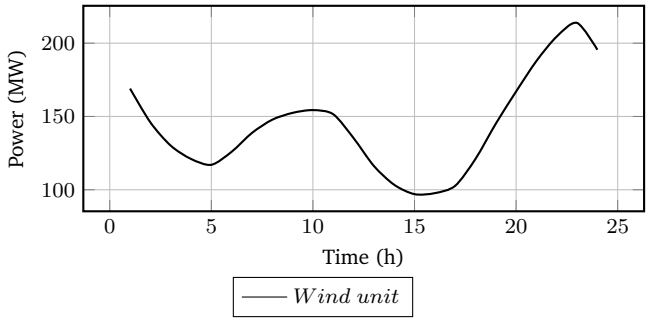

Figure 5.33: Power produced by wind unit (Model V, case II)

less than when $\zeta = 60\%$ (See Figures 5.41 and 5.42).

The behavior of quantile function of load demand is a bit different (see Figure 5.45). In this case, if it is required to increase the probability of holding constraint (4.42), the value of $Q(p)$ increases which makes the value of load demand be larger when $\zeta = 80\%$ compared to when $\zeta = 60\%$. Figure 5.39

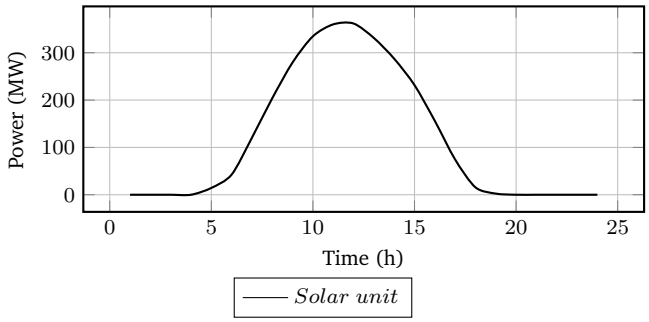

Figure 5.34: Power produced by solar unit (Model V, case II)

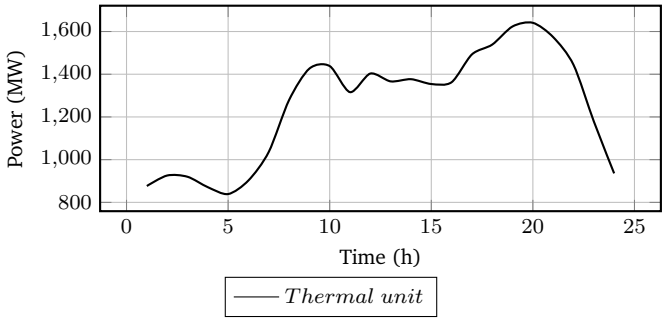

Figure 5.35: Power produced by thermal unit (Model V, case II)

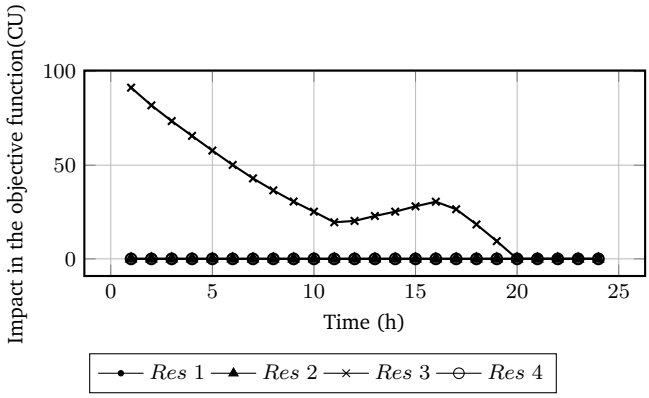

Figure 5.36: Dual variable of spillage (Model V, case II)

depicts this behavior.

Consequently, it is not difficult to see that, under this approach, the generation of renewable sources is underestimated and the load is overestimated

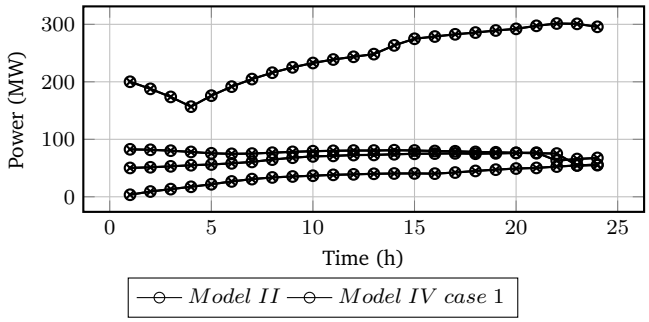

Figure 5.37: Comparison hydro power Model II and Model IV case I

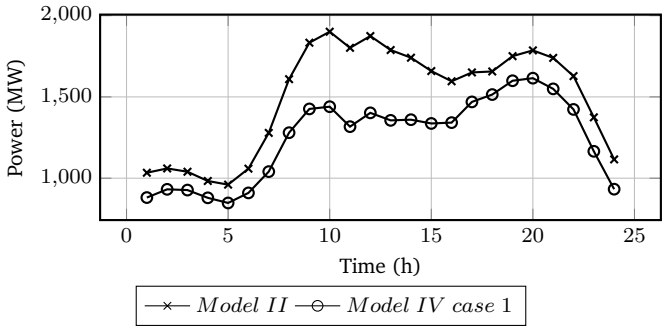

Figure 5.38: Comparison thermal power Model II and Model IV case I

Model	Objective function value (CU)	CPU Time (s)
Model IV case I	772725	22.7813
Model IV case II	776038	26.4063
Model V case I $\zeta = 80\%$	842719	25.6563
Model V case II $\zeta = 60\%$	777291	24.1563

Table 5.3: Minimum operation costs.

in order to ensure that the generated power is going to supply the consumed power. This behavior impacts the objective function as Table 5.4 shows. The reason for this is that, when the renewable source production decreases and the load increases, the thermal unit has to produce more in order to keep the power balance as Figure 5.40 depicts. Thereby, the operation cost are higher.

It addition, it can be seen that, for the Model IV, case I and the case with $\zeta = 60\%$, the values of solar power and power consumed are similar, likewise wind power for both cases are comparable, with a gap between 0 and 11 hours. This implies that using mean values of data to carry out the scheduling is an

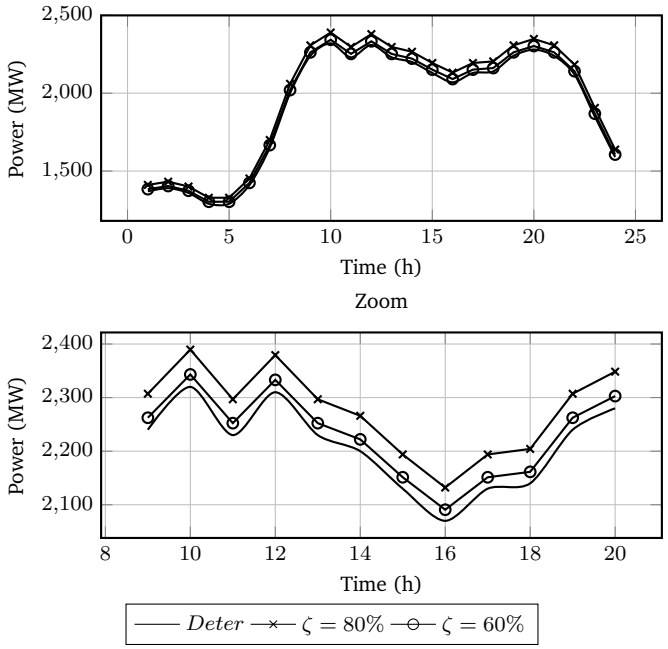

Figure 5.39: Power consumed in all 3 cases

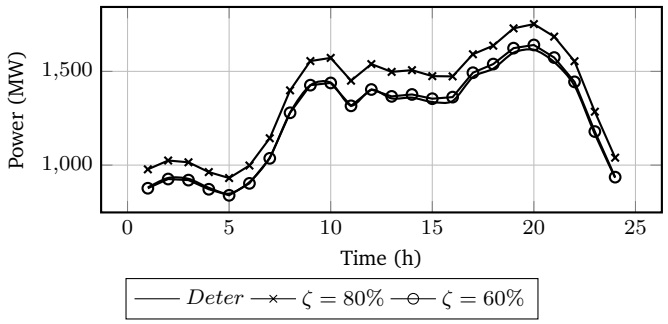

Figure 5.40: Power produced by thermal unit in all 3 cases

assumption that only allows values around 60% of robustness.

5.5 Summary of results

- The proposed SOC approximation for the STHS gives an optimum of 925866.00 CU with a convergence time of 4.7 S. This value of the objective function is between the range of results of other algorithms that

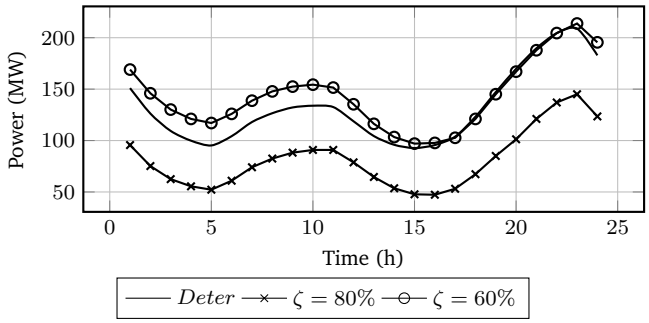

Figure 5.41: Power produced by twind unit in all 3 cases

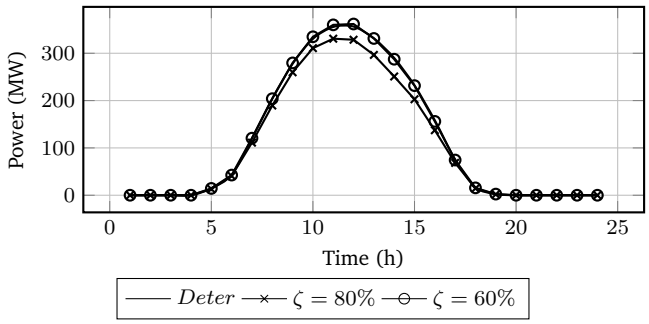

Figure 5.42: Power produced by solar unit in all 3 cases

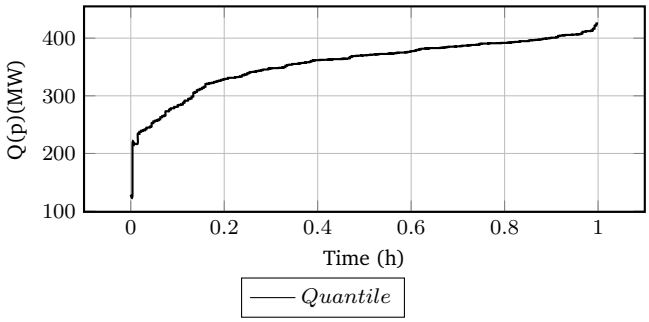

Figure 5.43: Quantile function of solar power at 12 pm

do not consider rigorous mathematics. Comparing these results gives us a good idea regarding how close the proposed methodology is to the optimum.

- The impact of renewable energy integration in a traditional hydrothermal system is analyzed. Thus, the generation costs reduce 16.5 % (Model IV case I), 16.1 % (Model IV case II), 8.9 % (Model V case I) and 16 % (Model

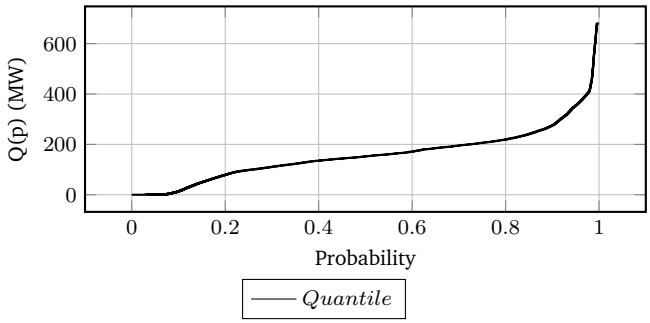

Figure 5.44: Quantile function of wind power at 12 pm

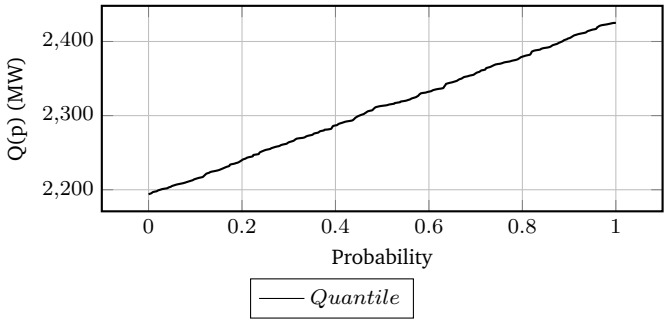

Figure 5.45: Quantile function of load demand at 12 pm

V case II), in comparison to results obtained by Model II.

- The spillage of reservoir 3 tends to be $2 \times 10^4 \frac{m^3}{s}$ as much as possible. These can be explained under two approaches: First, the higher efficiency of unit 4 compared to unit 3 makes the optimization model produce more power with unit 4 instead of unit 3, which promotes spilling water from reservoir 3 to reservoir 4. Second, by analyzing the dual variable of upper spillage, it is observed that these constraints impact the objective function considerably (see Figures 5.9, 5.18, 5.27 and 5.36).
- The lines capability can affect the operation of the system. Thus, the operation costs increase from 772725 CU (Model IV case I) to 776038 CU (Model IV case II). Furthermore, the operation of its reservoirs was also affected.
- Since the main values of wind speed and solar irradiation only ensure a robustness close 60% (Figures 5.41 and 5.42), these measures are an inaccurate methodology to predict the power produced by renewable energy.
- As higher robustness is considered, lower renewable generation and higher demand values are obtained, which implies higher production costs.

Chapter 6

Conclusions and future works

6.1 Conclusions

- A SOC relaxation was carried out which showed a superior performance (faster CPU time) compared to several heuristic techniques studied before. Besides, it is much simpler than the SDP relaxation presented in previous studies.
- It was confirmed that convex relaxation gives a global optimum for the approximated short-term hydrothermal coordination model, something that is not possible to find when heuristics algorithms are used.
- The dual variable of upper limit of spillage was analyzed. It was found that the spillage should not be ignored in this problem, since the study of its dual variable shows that it affects the objective function considerably when hydro-chains are considered. It is important to highlight that this kind of analysis cannot be carried out with heuristic and metaheuristic tecniques.
- A robust model which considers the stochasticity of the renewable sources and load demand was developed by modeling the power produced at generator nodes as chance constraints. This methodology turns out to be conservative for wind generation due to the shape of its quantile function, which increases slowly as probability increases. In doing so, a scenarios approach can be more suitable when it comes to wind power. Contrariwise, the quantile function of solar power increases faster, which results in a not-so-conservative deterministic equivalent for the constraint related to power produced by solar units. Futhermore, the robustness of load demand, under this approach, vary in a linear way in a small interval, this makes sense if the high accuracy of load prediction and its normal distribution are considered.

- It was observed that using the mean value of data of the stochastic variables does not represent the real behavior of said variables. Since, by using this, just a robustness around of 60% can be guaranteed.
- The impact of the transmission grid on the scheduling problem was studied. Results show that a contingency of key transmission lines can affect not only the generation scheduling but also the operation of reservoirs.

6.2 Future works

- To include energy storage devices in the problem.
- To consider the unit commitment.
- To study the correlation between solar radiation, wind speed and inflows can be proposed in order to have a more accurate model.
- To consider market prices in the problem.
- To analysis the valve effect of the thermal units.

Appendix A

Test system

The system used to evaluate the performance of the proposed methodology consists of a multi-chain cascade of 4 hydro units,a number of thermal units represented by an equivalent thermal plant, a photovoltaic solar farm and a wind farm. Additionally, the new England IEEE-39 bus system was considered in order to study the performance of the algorithm when the grid is taken into account. The characteristics of the test system are presented bellow.

A.1 Characteristics of load, hydro and thermal units

Plant	V_{min}	V_{max}	V_{ini}	V_{end}	Q_{min}	Q_{max}	PH_{min}	PH_{max}	S_{min}	S_{max}
1	80	150	100	120	5	15	0	500	0	2
2	60	120	80	80	6	15	0	500	0	2
3	100	240	170	170	10	30	0	500	0	2
4	70	160	120	120	13	25	0	500	0	2

Table A.1: Reservoir storage capacity limits, plant discharge limits, reservoir end conditions, spillage bounds $(10^4 m^3)$ and plant generation limits (MW)

Plant	C_1	C_2	C_3	C_4	C_5	C_6
1	-0.0042	-0.42	0.030	0.90	10	-50
2	-0.0040	-0.30	0.015	1.14	9.5	-70
3	-0.0016	-0.30	0.014	0.55	5.5	-40
4	-0.0030	-0.31	0.027	1.44	14	-90

Table A.2: Hydropower coefficients

Plant	1	2	3	4
R_u	0	0	2	1
τ_d	2	3	4	0

Table A.3: Number of up stream plants R_u and time delay to immediate downstream plant τ_d

.

Hour	I_{R_1}	I_{R_2}	I_{R_3}	I_{R1_4}	Load
1	10	8	8.1	2.8	1370
2	9	8	8.2	2.4	1390
3	8	9	4	1.6	1360
4	7	9	2	0	1290
5	6	8	3	0	1290
6	7	7	4	0	1410
7	8	6	3	0	1650
8	9	7	2	0	2000
9	10	8	1	0	2240
10	11	9	1	0	2320
11	12	9	1	0	2230
12	10	8	2	0	2310
13	11	8	4	0	2230
14	12	9	3	0	2200
15	11	9	3	0	2130
16	10	8	2	0	2070
17	9	7	2	0	2130
18	8	6	2	0	2140
19	7	7	1	0	2240
20	6	8	1	0	2280
21	7	9	2	0	2240
22	8	9	2	0	2120
23	9	8	1	0	1850
24	10	8	0	0	1590

Table A.4: Reservoir Inflows ($10^4 m^3$) and Load demand (MW)

.

$P_{Th_{min}}(MW)$	$P_{Th_{max}}(MW)$	α	β	γ
20	2500	5000	19.2	0.002

Table A.5: parameters of thermal unit.

A.2 Characteristic of wind and solar farms

The wind farm considered in this test systems consists of 340 wind turbines. Their characteristics are presented in Table A.6. On the other hand, the solar farm consists of 2500000 photovoltaic panels, each one with rated power

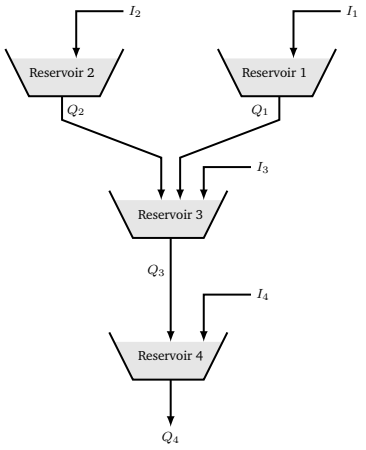

Figure A.1: Hydraulic system test network. Data for this test system is available in (Orero and Irving, 1998)

equal to 240 watts which adds a nominal power for the solar farm equal to 600 megawatts.

$P_{w_{rated}}(MW)$	$v_{cut-in}\ (m/s)$	v_{rated}	$v_{cut-out}\ (m/s)$
2	4	12	25

Table A.6: Characteristics of wind farm

Quantile function of solar power was built with capacity factor data taken from (Victoria and Andresen, 2019). These data belong to the recorded hourly data for every month of june between the years 1979 and 2017 in Spain. Said data correspond to units with solar tracker.

Wind speed data used to build the quantile function of wind power were taken from the wind prospector of The National Renewable Energy Laboratory of The United States. These data belong to the recorded hourly data for June in Hawai.

A.3 Characteristics of grid

The grid considered was taken from (Padiyar, 2008), Table A.3 shows the reactance values in per unit. In addition, the total load for each interval of time was distributed at all nodes in the proportion presented in Table A.3.

It is important to recall that generators 1,8,3 and 4 correspond to the hydro units 1,2,3 and 4, respectively; generator 10 corresponds to the thermal unit;

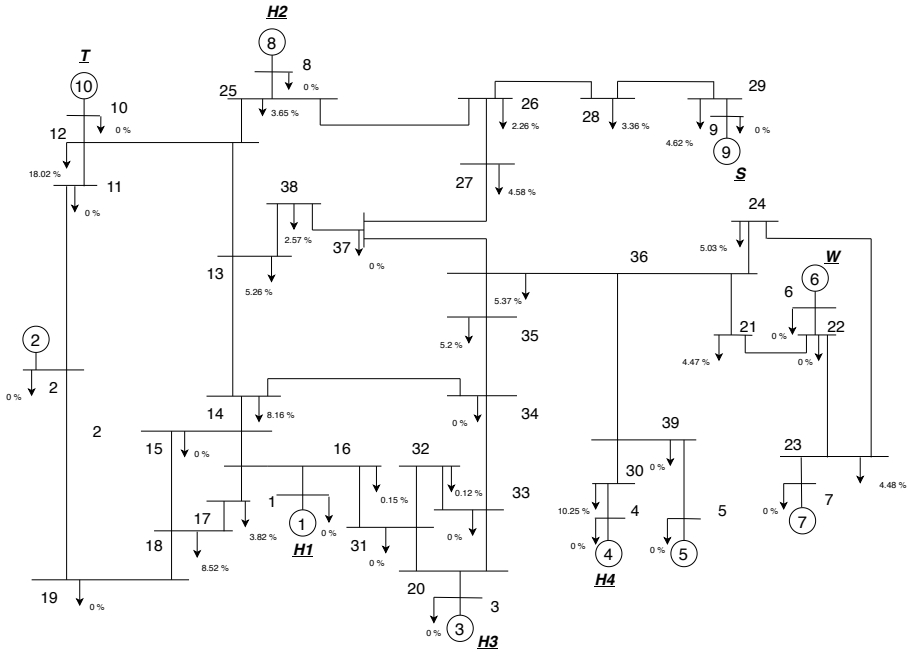

Figure A.2: New England, IEEE 39 Bus-system

generator 6 corresponds to the wind farm and generator 9 corresponds to the solar farm, the other generators are not considered.

Initial node	Final node	$X_{kn_{P.U}}$
37	27	0.0173
37	38	0.0082
36	24	0.0059
36	21	0.0135
36	39	0.0195
36	37	0.0089
35	36	0.0094
34	35	0.0217
33	34	0.0101
28	29	0.0151
26	29	0.0625
26	28	0.0474
26	27	0.0147
25	26	0.0323
23	24	0.0350
22	23	0.0096
21	22	0.0135
20	33	0.0043
20	31	0.0043
19	2	0.0250
18	19	0.0363
17	18	0.0046
16	31	0.0082
16	17	0.0092
15	18	0.0112
15	16	0.0026
14	34	0.0129
14	15	0.0128
13	38	0.0133
13	14	0.0213
12	25	0.0086
12	13	0.0151
11	12	0.0411
11	2	0.0250

Table A.7: Reactance of lines in P.U

Initial node	Final node	$X_{kn_{P.U}}$
39	30	0.0138
39	5	0.0142
32	33	0.0435
32	31	0.0435
30	4	0.018
29	9	0.0156
25	8	0.0232
23	7	0.0272
22	6	0.0143
20	3	0.02
16	1	0.025
12	10	0.0181

Table A.8: Reactance of transformers

Node	Percentage of total load [%]
1	0
2	0
3	0
4	0
5	0
6	0
7	0
8	0
9	0
10	0
11	0
12	0.1802
13	0.0526
14	0.0816
15	0
16	0.0015
17	0.0382
18	0.0852
19	0
20	0
21	0.0447
22	0
23	0.0448
24	0.0504
25	0.0366
26	0.0227
27	0.0458
28	0.0336
29	0.0462
30	0.1025
31	0
32	0.0012
33	0
34	0
35	0.0522
36	0.0537
37	0
38	0.0257
39	0

Table A.9: Distribution of load

Appendix B

Brief review of convex optimization

B.1 Convex set

A set Ω in $\mathbb{R}^n$ is convex if for any points $\mathfrak{X}, \mathfrak{Y} \in \Omega$ there is a point $\mathfrak{Z}$ given by:

$$\mathfrak{Z} = (1 - \lambda)\mathfrak{X} + \lambda\mathfrak{Y} \tag{B.1}$$

Such as $\mathfrak{Z} \in \Omega$ with $\lambda \in \mathbb{R}^n$, $0 \leq \lambda \ \leq 1$.

This definition can be extended to several points. If the convex set $\Omega \in \mathbb{R}^n$ with $\mathfrak{X}_k \in \Omega$ and $\alpha_k \in \mathbb{R}^n$ is convex, then $\sum \alpha_k \mathfrak{X}_k \in \Omega$ if $\sum \alpha_k = 1$.

Figure B.1 depicts how the aforementioned condition is true for two points belonging to Ω_a, whereas in Ω_b there are points that belong to the line but they are out of the space; thereby Ω_a is convex while Ω_b is not convex.

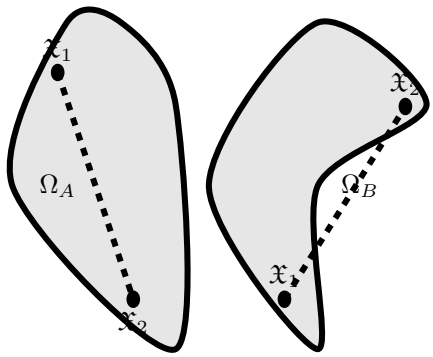

Figure B.1: Convex and non-convex set

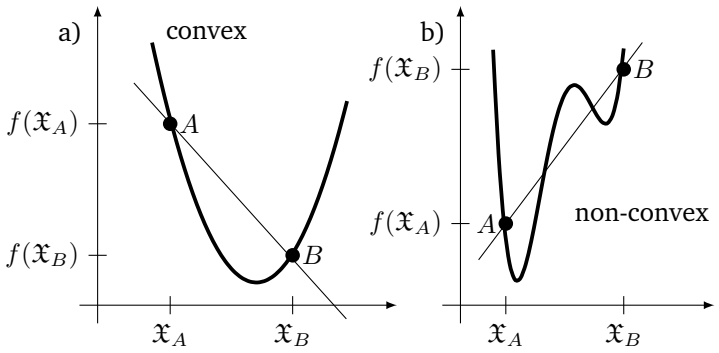

Figure B.2: Convex and non-convex functions

B.2 Convex function

A function $f : \mathbb{R}^n \to \mathbb{R}$ is convex if the domain of f is a convex set and if for all $\mathfrak{X}, \mathfrak{Y} \in \mathbf{dom} f$, and λ with $0 \leq \lambda \leq 1$, we have (Boyd and Vndenberghe, 2009):

$$f(\lambda\mathfrak{X} + (1-\lambda)\mathfrak{Y}) \leq \lambda f(\mathfrak{X}) + (1-\lambda) f(\mathfrak{Y}) \tag{B.2}$$

Equation (B.2) can be written as:

$$f(\alpha\mathfrak{X} + \beta y) \leq \alpha f(\mathfrak{X}) + \beta f(\mathfrak{Y}) \tag{B.3}$$

B.3 Convex problem

A convex optimization problem is of the form:

$$\text{minimize } f_0(\mathfrak{X}) \tag{B.4}$$
$$\text{subject to } f_i(\mathfrak{X}) \leq 0 \tag{B.5}$$
$$h_i(\mathfrak{X}) = 0 \tag{B.6}$$

Where $f_0(\mathfrak{X})$ and $f_i(\mathfrak{X})$ are convex and $h_i(\mathfrak{X})$ is an affine function of the structure $a_i^T \mathfrak{X} = b_i$ (Boyd and Vndenberghe, 2009)

B.4 Uniqueness and globality

Convex optimization is a field which has been explored intensively recently due to two main characteristics (Boyd and Vndenberghe, 2009):

A. If a problem is convex, it implies that the same optimum is going to be achieve regardless the number of times that the optimization process is carried out (uniqueness characteristic).

B. In a convex problem it is easy to see that it only has an optimum operation point (see Figure B.2). Thus, the convex optimization process guarantee the globality of the found solution (globality characteristic).

Both, uniqueness and globality are always desired in all optimization process.

Appendix C

Probability space definitions

C.1 Sample space H

For the purpose of modeling systems that produce uncertain or random measurements, let us define H as the set of all possible distinct, indecomposable measurements (outcomes) that could be observed (Gubner, 2006). That is to say, H is the set of all possible outcomes of a random experiment.

C.2 Outcomes and events

Elements or points in the sample space H are called outcomes. Collections of outcomes are called events. Therefore, an event is a subset of the sample space (Gubner, 2006).

C.3 $\sigma-$algebra $\mathfrak{B}$

Let H be an abstract space, that is with no special structure. Let 2^H denote all subsets of H, including the empty set denoted by $\emptyset$. With $\mathfrak{B}$ being a subset of 2^H. If $\mathfrak{B}$ satisfies the the following properties:

A. $\emptyset \in \mathfrak{B}$ and $H \in \mathfrak{B}$.

B. If $B \in \mathfrak{B}$ then $B^C \in \mathfrak{B}$, where B^C represents the complement of B.

C. $\mathfrak{B}$ is closed under countable unions and intersections: that is to say, if B_1, B_2, B_3... is a countable sequence of events in $\mathfrak{B}$, then $\cup_{i=1}^{\infty} B_i$ and $\cap_{i=1}^{\infty} B_i$ are both also in $\mathfrak{B}$.

then $\mathfrak{B}$ is defined as a $\sigma-$algebra (Jacod and Protter, 2004). In brief, a set that contains other subsets, the unions of the subsets and their intersessions, is what we call a $\sigma-$algebra.

C.4 Probability measure function $\mathfrak{P}$

Given a sample space H, and a function $\mathfrak{P}$ defined on the subsets of H. We define a probability measure $\mathfrak{P}$ if the following axioms are satisfied:

A. The empty set $\emptyset$ is called the impossible event. The probability of this event is zero; i.e., $\mathfrak{P}(\emptyset) = 0$.

B. Probabilities are nonnegative; i.e., for any event B, $\mathfrak{P}(B) \geq 0$

C. If B_1, B_2, B_3... are events that are mutually exclusive, i.e., $B_n \cap B_m = \emptyset$ for $n \neq m$ then:

$$\mathfrak{P}(\bigcup_{n=1}^{\infty} B_n) = \sum_{n=1}^{\infty} \mathfrak{P}(B_n) \tag{C.1}$$

D. The probability of the entire sample space (sure event) is one; i.e $\mathfrak{P}(H) = 1$. If an event $B \neq H$ satisfies $\mathfrak{P}(B) = 1$, then B is an almost-sure event.

This is to say, a probability distribution function is a measure that assigns a value to all subsets of the sample space such as that the value 1 is assigned to the whole sample space and the value zero is assigned to the empty set $\emptyset$. Moreover, the measure of a subset plus the measure of another subset is the measure of the union of both subsets.

Appendix D

linearization of the problem

In order to analyze the loss of information when linearizations are carried out for the STHTS problem, the Matlab curve fitting tool was used to carry out linear approximations of the hydropower equations. Thus, said equations take the following structure:

$$P_{H_L}^{j,t} = C_{1_L}^{j} V^{i,t} + C_{2_L}^{j} Q^{i,t} + C_{3_L}^{j} \tag{D.1}$$

Where the coefficients of the linearization are given by the Table:

Plant	C_{1_L}	C_{2_L}	C_{3_L}
1	0.5775	4.55	-21.97
2	0.234	5.05	7.755
3	0.286	-4.12	65.92
4	1.263	5.325	-3.222

Table D.1: Hydropower coefficients linearization

It is worth mentioning that the linearizations were carried out for the intervals between $Q_{min} - Q_{max}$ and $V_{min} - V_{max}$. Besides, the linearization used was a polynomial one.

Figures D.1 and D.2 presents the water discharges and the volumes of reservoirs obtained when (D.1) is considered. These values were replaced in both, Equation (D.1) and Equation (2.8) obtaining the power produced for all units in both cases (Tables D.2 and D.3). In doing so, results show a considerable difference between the power produced with the non-convex equation and the linear equation, when the values of Figures D.1 and D.2 are considered (Table D.4).

It is worth mentioning that the hydropower difference between the linear equations and the results of the quadratic equation are close of $20\|; MW$ (Table D.4) in most time intervals, which sums a total difference in a day of

536.87 MW. This gap is considerable if we take into account the size of the test system, and gives us an idea about how much information can be lost when linearizations are carried out. In addition, the values of volumes and water discharges for unit 3 in the first 5 hours, provided by the linearized model, gives negative values when they are replaced in the quadratic equation that models the real behavior of this unit (see Table D.3). This implies that the linearized model is giving non-feasible operation points since these negative values would mean that unit 3 is working as a pump that consumes power.

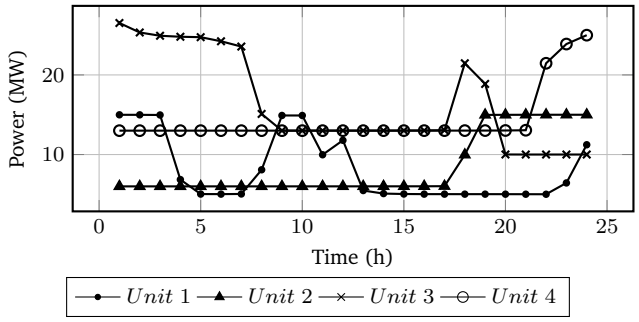

Figure D.1: Water discharge of hydro units hydro units (linearized model)

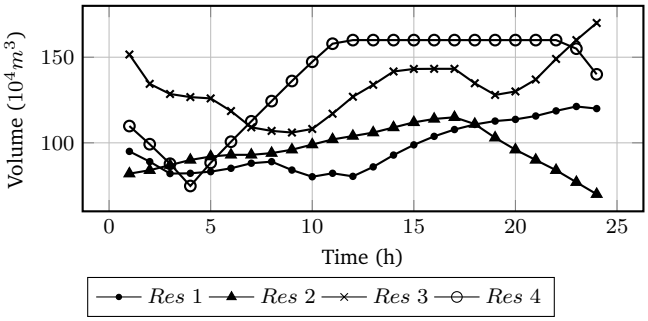

Figure D.2: Volumes of reservoirs (Linearized model)

Hour	$P^1_{H_L}$	$P^2_{H_L}$	$P^3_{H_L}$	$P^4_{H_L}$
1	105.6932	52.6906	0.0062	204.6809
2	104.2675	53.8450	0.0069	191.2934
3	102.5468	55.5769	0.0078	176.8956
4	61.5994	57.3089	0.0092	160.4768
5	52.6454	58.4635	0.0114	177.5541
6	53.0680	59.0409	0.0162	193.1292
7	53.8579	59.0410	0.0309	208.1842
8	69.4197	59.6189	34.2951	223.0804
9	102.7140	60.7744	42.6685	237.9085
10	101.7906	62.5072	43.2688	252.0888
11	77.3563	64.2397	45.8071	265.4297
12	86.1090	65.3960	48.6439	268.0867
13	55.5356	66.5521	50.6290	268.0880
14	55.2227	68.2870	52.8507	268.0888
15	56.3398	70.0235	53.2542	268.0925
16	57.4286	71.1879	53.2365	268.0941
17	58.3534	71.8122	53.1094	268.1005
18	59.0370	87.4615	16.0472	268.1090
19	59.5018	105.6468	24.7828	268.1303
20	59.7152	101.6503	61.8656	268.1823
21	60.1614	98.2153	63.8951	268.3506
22	60.8363	94.7695	67.3256	313.1363
23	68.6142	90.7320	70.4712	319.6652
24	92.5393	86.6933	73.3307	306.6811

Table D.2: Power produced by hydro units using linearized equations [MW].

Hour	$P^1_{H_Q}$	$P^2_{H_Q}$	$P^3_{H_Q}$	$P^4_{H_Q}$
1	95.8476	50.1732	-2.2545	200.0943
2	92.3943	51.3047	-0.4761	187.7564
3	87.9989	52.9424	-0.1429	173.7349
4	61.3087	54.5082	-0.0684	156.7936
5	48.0690	55.5122	-0.0376	174.3935
6	48.6838	56.0028	0.1007	189.4890
7	49.8031	56.0037	-0.0403	203.2134
8	71.8260	56.4874	37.7835	215.9544
9	89.3310	57.4297	40.4192	227.8087
10	86.7649	58.7822	41.2324	238.3724
11	78.1599	60.0626	44.5423	247.6220
12	83.1812	60.8794	47.9279	249.3908
13	52.6362	61.6647	50.1211	249.3925
14	51.6135	62.7837	52.3878	249.3950
15	52.6128	63.8349	52.7934	249.4008
16	53.4774	64.5114	52.8127	249.4048
17	54.1132	64.9213	52.8022	249.4165
18	54.4862	88.7248	25.4222	249.4330
19	54.7124	103.0983	34.9574	249.4735
20	54.7815	99.1402	47.6731	249.5728
21	54.9221	95.4299	49.5010	249.8970
22	55.0753	91.4254	52.2900	313.9870
23	67.7341	86.3820	54.4429	318.5734
24	97.2746	80.9460	56.0642	303.5320

Table D.3: Power produced by hydro units using quadratic equations [MW].

Hour	TP_{H_L}	TP_{H_Q}	***HPDLQ***
1	363.0708	343.8607	19.2101
2	349.4127	330.9794	18.4334
3	335.0271	314.5332	20.4939
4	279.3943	272.5422	6.8521
5	288.6744	277.9371	10.7373
6	305.2543	294.2763	10.9780
7	321.1140	308.9799	12.1341
8	386.4140	382.0512	4.3628
9	444.0653	414.9886	29.0767
10	459.6554	425.1520	34.5034
11	452.8328	430.3867	22.4461
12	468.2356	441.3793	26.8563
13	440.8046	413.8145	26.9901
14	444.4492	416.1800	28.2691
15	447.7101	418.6420	29.0681
16	449.9471	420.2062	29.7409
17	451.3755	421.2532	30.1223
18	430.6547	418.0661	12.5886
19	458.0617	442.2417	15.8200
20	491.4135	451.1677	40.2458
21	490.6224	449.7501	40.8723
22	536.0677	512.7777	23.2900
23	549.4827	527.1324	22.3503
24	559.2444	537.8169	21.4275

Table D.4: Total hydropower using linearized equations, Total hydropower using quadratic equation and difference between the total hydropower using linearized equations and the total hydropower using quadratic equations [MW].

Bibliography

Aharon Ben-Tal, L. E. G. and Nemirovski, A. (2009). *Robust Optimization*. Princeton University Press.

Alizadeh, F. and Goldfarb, D. (2003). Second-order cone programming. *Mathematical Programming*, 95:3–51.

Amirarslan Haghrah, B. M.-i. and Seyedmonir, S. (2015). Real coded genetic algorithm approach with random transfer vectors-based mutation for short-term hydro–thermal scheduling. *IET Generation, Transmission and Distribution*, 9:75–89.

Amjady, N. and Nasiri-Rad, H. (2009). Nonconvex economic dispatch with ac constraints by a new real coded genetic algorithm. *IEEE Transactions on Power Systems*, 24:1489–1501.

Amjady, N. and Soleymanpour, H. R. (2010). Daily hydrothermal generation scheduling by a new modified adaptive particle swarm optimization technique. *Electric Power Systems Research*, 80:723–732.

Andre Luiz Diniz, M. E. P. M. (2008). A four-dimensional model of hydro generation for the short-term hydrothermal dispatch problem considering head and spillage effects. *IEEE Transactions on Power Systems*, 23:1298–1308.

A.Rasoulzadeh-akhijahani and Mohammadi-ivatloo, B. (2015). Short-term hydrothermal generation scheduling by a modified dynamic neighborhood learning based particle swarm optimization. *International Journal of Electrical Power and Energy Systemsl*, 67:350–367.

B. Yu, X. Y. and Wang, J. (2007). Short-term hydro-thermal scheduling using particle swarm optimization method. *Energy Convers. Manag.*, 48:1902–1908.

Basu (2016). Quasi-oppositional group search optimization for hydrothermal power system. *International Journal of Electrical Power and Energy Systems*, 81:324–335.

Basu, M. (2014). Improved differential evolution for short-term hydrothermal scheduling. *Electrical Power and Energy Systems*, 58:91–100.

Basu, M. (2019). Dynamic economic dispatch with demand-side management incorporating renewable energy sources and pumped hydroelectric energy storage. *Soft Computing*, 101:877–893.

Beatriz P. Cotiaa, C. L. B. and Dinizb, A. L. (2019). Optimization of wind power generation to minimize operation costs in the daily scheduling of hydrothermal systems. *Electrical Power and Energy Systems*, 113:539–548.

Boyd, S. and Vndenberghe, L. (2009). *Convex Optimization*. Cambridge University Press.

Bram L. Gorissen, Y. and den Hertog, D. (2015). A practical guide to robust optimization. *Omega*, 53:124–137.

Chaoshun Li, W. W. and Chen, D. (2019). Multi-objective complementary scheduling of hydro-thermal-re power system via a multi-objective hybrid grey wolf optimizer. *Energy*, 171:241–255.

Chen, P.-H. and Chang, H.-C. (1996). Genetic aided scheduling of hydraulically coupled plants in hydro-thermal coordination. *IEEE Transactions on Power Systems*, 11:975–981.

Chen, R. L. Y. L. Y. (2016). A virus-evolutionary differentiated-pso approach for short-term generation scheduling with uncertainties. *International Transactions on Electrical Energy Systems*, 26:2288–2307.

Christensen, G. S. and El-Hawary, M. E. (1979). *Optimal Economic Operation of Electric Power Systems*. Academic Press, INC.

Chunlong Li, J. Z. and Peng Lu, C. W. (2015). Short-term economic environmental hydrothermal scheduling using improved multi-objective gravitational search algorithm. *Energy Conversion and Management*, 89:127–136.

Damodaran, S. K. and Kumar, T. K. S. (2018). Hydro-thermal-wind generation scheduling considering economic and environmental factors using heuristic algorithms. *energies*.

del Mar Rubio, M. and Tafunell, X. (2014). Latin american hydropower: A century of uneven evolution. *Renewable and Sustainable Energy Reviews*, 138:323–334.

Deng, T.-B. (2011). Minimax design of low-complexity even-order variable fractional-delay filters using second-order cone programming. *IEEE Transaction on Circuits and Systems II*, 58:692–696.

E. Gil, J. B. and Rudnick, H. (1264). Short-term hydrothermal generation scheduling model using a genetic algorithm. *IEEE Transactions on Power Systems*, 18:1256.

Fabricio Y.K. Takigawa, Edson L. da Silva, E. C. F. and Rodrigues, R. N. (2012). Solving the hydrothermal scheduling problem considering network constraints. *Electric Power Systems Research*, 88:89–97.

Fang Chen, Jianzhong Zhou, C. W. C. L. and Lu, P. (2017). A modified gravitational search algorithm based on a non-dominated sorting genetic approach for hydro-thermal-wind economic emission dispatching. *Energy*, 121:276–291.

Farhat, I. A. and El-Hawary, M. E. (2009). Optimization methods applied for solving the short-term hydrothermal coordination problem. *Electric Power Systems Research*, 79:1308–1320.

Fuentes-Loyola and Quintana, V. (2003). Medium-term hydrothermal coordination by semidefinite programming. *IEEE Transactions on Power Systems*, 18:1515–1522.

Gil, E. and Araya, J. (2016). Short-term hydrothermal generation scheduling using a parallelized stochastic mixed-integer linear programming algorithm. *Energy Procedia*, 171:77–84.

Gilchrist, W. G. (2000). *Statical Modelling with Quantile Functions*. CHAPMAN and HALL/CRC.

Gouthamkumar Nadakuditi, V. S. and Naresh, R. (2016). Application of non-dominated sorting gravitational search algorithm with disruption operator for stochastic multiobjective short term hydrothermal scheduling. *IET Generation, Transmission and Distribution*, 10:862 – 872.

Grainger, J. J. and Jr., W. D. S. (1994). *Power System Analysis*. MacGraw-Hill.

Gubner, J. A. (2006). *Probabilitiy and Random Processes for Electrical And Computer Engineers*. Cambridge University Press.

Hari Mohan Dubey, M. P. and Panigrahi, B. K. (2016). Ant lion optimization for short-term wind integrated hydrothermal power generation scheduling. *International Journal of Electrical Power and Energy Systems*, 83:158–174.

Haroon, S. S. and Malik, T. N. (2017). Short-term hydrothermal coordination using water cycle algorithm with evaporation rate. *International Transactions on Electrical Energy Systems*, 27(8).

Houzhong Yan, P. B. L. and Guan, X. (1993). Scheduling of hydrothermal power systems. *IEEE Transactions on Power Systems*, 8:1358–1365.

IEA (2019). Renewables 2019, market analysis and forecast from 2019 to 2024. https://www.iea.org/reports/renewables-2019. Accessed:2020-01-05.

Isabela Alves de Oliveira, R. S. and Szklo, A. (2017). The impact of energy storage in power systems: The case of brazil's northeastern grid. *Energy*, 122:50–61.

J. Zhang, J. and Yue, C. (2012). Small population-based particle swarm optimization for short-term hydrothermal scheduling. *IEEE Transactions on Power Systems.*, 27:142–152.

Jacod, J. and Protter, P. (2004). *Probabilitiy Essentials*. Springer.

Jan Machowski, Janusz W. Bialek, J. R. B. (2008). *Power system dynamics: and stability and control*. John Wiley and Sons.

Jarnail S. Dhillon, J. D. and Kothary, D. (2011). Real code genetic algorithm for stochastic hydrothermal generation scheduling. *Journal of Systems Science and Systems Engineering*, 20:87–109.

Jianzhong Zhou, Peng Lu, Y. L. C. W. and Mo, L. (2016). Short-term hydrothermal-wind complementary scheduling considering uncertainty of wind power using an enhanced multi-objective bee colony optimization algorithm. *Energy Conversion and Management*, 123:116–129.

Jiehong Kong, H. I. S. and Fosso, O. B. (2020). An overview on formulations and optimization methods for the unit-based short-term hydro scheduling problem. *Electric Power Systems Research*, 178:1–14.

Jinbao Jian, S. P. and Yang, L. (2019). Solution for short-term hydrothermal scheduling with a logarithmic size mixed-integer linear programming formulation. *Energy*, 171:770–784.

Jing Liu, A.B. Gershman, Z.-Q. L. and Wong, K. M. (2003). Adaptive beamforming with sidelobe control. *IEEE Signal Processing Letters*, 10:331–334.

J.P.S. Catalao, H. P. and Mendesb, V. (2010). Mixed-integer nonlinear approach for the optimal scheduling of a head-dependent hydro chain. *Electric Power Systems Research*, 80:935–942.

J.P.S. Catalao, H. P. a. and c, V. M. (2011). Hydro energy systems management in portugal: Profit-based evaluation of a mixed-integer nonlinear approach. *Energy*, 36:500–507.

J.Wood, A. and F.Wollenberg, B. (1996). *Power Generation, Operation, and Control*. John Wiley and Sons, INC.

Kothari, D. and Dhillon, J. (2007). *Power System Optimization*. Prentice-hall of India.

Kumar, S. and Naresh, R. (2007). Efficient real coded genetic algorithm to solve the non-convex hydrothermal scheduling problem. *International Journal of Electrical Power and Energy Systems*, 29:738–747.

kundur, P. (1994). *Power System Stability and Control*. McGraw-hill.

Lakshminarasimman, L. and Subramanian, S. (2006). Short-term scheduling of hydrothermal power system with cascaded reservoirs by using modified differential evolution. *IEE Proceedings - Generation, Transmission and Distribution*, 153:693–700.

Lakshminarasimman, L. and Subramanian, S. (2008). A modified hybrid differential evolution for short-term scheduling of hydrothermal power systems with cascaded reservoirs. *Energy Conversion and Management*, 49:2513–2521.

M. Nazari-Heris, B. M.-I. and Gharehpetian, G. B. (2017). Short-term scheduling of hydro-based power plants considering application of heuristic algorithms: A comprehensive review. *Renewable and Sustainable Energy Reviews*, 74:116–129.

Manda, K. K. and Chakraborty, N. (2008). Differential evolution technique-based short-term economic generation scheduling of hydrothermal systems. *Electric Power Systems Research*, 78:1972–1979.

Masters, G. M. (2004). *Renewable and Efficient Electric Power Systems*. John Wiley and Sons, INC.

Md. Sayeed Salam, K. M. N. and Hamdan, A. R. (1997). Hydrothermal scheduling based lagrangian relaxation approach to hydrothermal coordination. *IEE Proceedings - Generation, Transmission and Distribution*, 144:482–488.

Md. Sayeed Salam, K. M. N. and Hamdan, A. R. (1998). Comprehensive algorithm for hydrothermal coordination. *IEEE Transactions on Power Systems*, 13:226–235.

N. Gouthamkumar, V. S. and Naresh, R. (2015). Disruption based gravitational search algorithm for short term hydrothermal scheduling. *Expert Systems with Applications*, 42:15.

Nguyen, T. T. and Vo, D. N. (2017). Modified cuckoo search algorithm for multiobjective short-term hydrothermal scheduling. *Swarm and Evolutionary Computation*, 37:73–89.

Nidul Sinha, C. and Chattopadhyay, P. K. (2003). Fast evolutionary programming techniques for short-term hydrothermal scheduling. *IEEE Transactions on Poswer Systems*, 18:214–220.

Olimpo Anaya-Lara, Nick Jenkins, J. E. P. C. and Hughes, M. (2009). *Wind Energy Generation, Modeling and Control*. John Wiley and Sons.

Orero, S. and Irving, M. (1998). A genetic algorithm modelling framework and solution technique for short term optimal hydro-thermal scheduling. *IEEE Transactions on Power Systems*, 12:501–518.

P. K. Hota, R. C. and Chattopadhyay, P. K. (1999). Short-term hydrothermal scheduling through evolutionary programming technique. *Electric Power Systems Research*, 52:189–196.

Padiyar, K. R. (2008). *Power system dynamics and stability and control*. BS Publications.

Parrilla, E. and Garcıa-Gonzalez, J. (2006). Improving the bandb search for large-scale hydrothermal weekly scheduling problems. *Electrical Power and Energy Systems*, 28:339–348.

P.K. Hota, A. B. and Chakrabarti, R. (2009). An improved pso technique for short-term optimal hydrothermal scheduling. *Electric Power Systems Research.*, 79:1047–1053.

R. K. Swain, A. K. Barisal, P. K. H. and Chakrabarti, R. (2011). Short-term hydrothermal scheduling using clonal selection algorithm. *International Journal of Electrical Power and Energy Systems*, 33:647–656.

Rodrigues, R. N. and Edson L. da Silva, Erlon C. Finardi, F. Y. K. T. (2011). Solving the short-term scheduling problem of hydrothermal systems via lagrangian relaxation and augmented lagrangian. *Mathematical Problems in Engineering*, 12.

Ross, S. (1998). *A first course in probability*. Prentice-Hall, Inc.

Roy, P. K. (2013). Teaching learning based optimization for short-term hydrothermal scheduling problem considering valve point effect and prohibited discharge constraint. *International Journal of Electrical Power and Energy Systems*, 53:10–19.

Ruud Egging, A. T. (2016). Norway's role in the european energy transition. *Energy Strategy Reviews*, 20:99–101.

Ruzic, S. and Rajakovic, R. (1998). Optimal distance method for lagrangian multipliers updating in short-term hydro-thermal coordination. *IEEE Transactions on Power Systems*, 13:1439–1444.

S Vedula, P. P. M. (2007). *Water resources systems: Modelling and techniques and analysis*. Tata MacGraw-Hill.

Sasikala, J. and Ramaswamy, M. (2010). Optimal gamma based fixed head hydrothermal scheduling using genetic algorithm. *Expert Systems with Applications*, 37:3352–3357.

Schweizer, B. and Sklar, A. (2005). *Probabilistic Metric Spaces*. Dover publications, INC.

Sivasubramani, S. and Swarup, K. S. (2011). Hybrid de–sqp algorithm for non-convex short term hydrothermal scheduling problem. *Energy Conversion and Management*, 52:757–761.

Slodoban Ruzic, A. V. and Rajakovic, N. (1996). A flexible approach to short-term hydro-thermal coordination. ii. dual problem solution procedure. *IEEE Transactions on Power Systems*, 11:1572–1578.

Sorensen, K. (2015). Metaheuristics—the metaphor exposed. *International Transactions in Operational Research*, 22:3–18.

Spandan Thaker, Abayomi Olufemi Oni, E. G. and Kumar, A. (2019). Evaluating energy and greenhouse gas emission footprints of thermal energy storage systems for concentrated solar power applications. *Journal of Energy Storage*, 26.

Sujoy Das, A. B. and Chakraborty, A. K. (2018a). Fixed head short-term hydrothermal scheduling in presence of solar and wind power. *Energy Strategy Reviews*, 74:47–60.

Sujoy Das, A. B. and Chakraborty, A. K. (2018b). Solution of short-term hydrothermal scheduling problem using quasi-reflected symbiotic organisms search algorithm considering multi-fuel cost characteristics of thermal generator. *Arabian Journal for Science and Engineering*, 43(6):2931–2960.

Tiago Norbiato Santos, A. L. D. and Borges, C. L. T. (2017). A new nested benders decomposition strategy for parallel processing applied to the hydrothermal scheduling problem. *IEEE Transactions on Power Systems*, 8:1504–1512.

UPME (2019). Plan de expansion de referencia generacion transmision 2015 - 2029. https://www1.upme.gov.co/Paginas/Plan-Expansion-2015-2029.aspx. Accessed:2020-02-13.

Victoria, M. and Andresen, G. B. (2019). *Using validated reanalysis data to investigate the impact of the PV system configurations at high penetration levels in European countries, Progress in Photovoltaics: Research and Applications (2019)*. John Wiley and Sons, INC.

Xiaohui Yuan, Liang Wang, Y. Y. (2008). Application of enhanced pso approach to optimal scheduling of hydro system. *Energy Conversion and Management*, 49:2966–2972.

Xiaotao Wu, Yuehua Huang, H. T. and Yuan, X. (2014). An improved gravitational search algorithm for solving short-term economic/environmental hydrothermal scheduling. *Soft Computing volume*, 19.

Xuebin Wang, Jianxia Chang, X. M. and Wang, Y. (2018). Short-term hydro-thermal-wind-photovoltaic complementary operation of interconnected power systems. *Applied Energy*, 229:945–962.

Xuebin Wang, Jianxia Chang, X. M. and Wang, Y. (2019). Hydro-thermal-wind-photovoltaic coordinated operation considering the comprehensive utilization of reservoirs. *Energy Conversion and Management*, 198.

Yachao Zhang, Jian Le b, X. L. b. F. Z. a. K. L. b. and An, X. (2018). Multi-objective hydro-thermal-wind coordination scheduling integrated with large-scale electric vehicles using imopso. *Renewable Energy*, 128:91–107.

Yalcinoz, T. and Short, M. (1998). Neural networks approach for solving economic dispatch problem with transmission capacity constraints. *IEEE Transactions on Power Systems*, 13:307–313.

Ye Zhou, Yuan Tian, K. W. and Ghandhari, M. (2017). Robust optimisation for ac–dc power flow based on second-order cone programming. *The Journal Of Engineering*, 2017:2164 – 2167.

Yong-Gang Wu, C.-Y. H. and Wang, D.-Y. (2000). A diploid genetic approach to short-term scheduling of hydro-thermal system. *IEEE Transactions on Power Systems*, 15:1268–1274.

Yongqiang Wang, Jianzhong Zhou, L. M. R. Z. and Zhang, Y. (2012). Short-term hydrothermal generation scheduling using differential real-coded quantum-inspired evolutionary algorithm. *Energy*, 44:657–671.

Youlin Lu, Jianzhong Zhou, H. Q. Y. W. and Zhang, Y. (2010). An adaptive chaotic differential evolution for the short-term hydrothermal generation scheduling problem. *Energy Conversion and Management*, 51:1481–1490.

Yuan, X., Tian, H., Yuan, Y., Huang, Y., and Ikram, R. M. (2015). An extended nsga-iii for solution multi-objective hydro-thermal-wind scheduling considering wind power cost. *Energy Conversion and Management*, 96:568–578.

Yunan Zhu, Jinbao Jian, J. W. and Yang, L. (2013). Global optimization of non-convex hydro-thermal coordination based on semidefinite programming. *IEEE Transactions on Power Systems*, 28:3720 – 3728.

Yuqiang Wua, Y. W. and Liu, X. (2019). Couple-based particle swarm optimization for short-term hydrothermal scheduling. *Applied Soft Computing Journal*, 74:440–450.

Z. Yu, F.T. Sparrow, B. B. and Smardo, F. (2000). On convexity issues of short-term hydrothermal scheduling. *Electrical Power and Energy Systems*, 26:451–457.